NASA TECHNICAL MEMORANDUM

NASA TM X-71679

NASA TM X-71679

(NASA-TM-X-71679) COMPARISON OF PARAMETRIC DUCT-BURNING TURBOFAN AND NON-AFTERBURNING TURBOJET ENGINES IN A MACH 2.7 TRANSPORT (NASA) 73 p HC $4.25 CSCL 21E

N75-19247

Unclas

G3/07 13422

COMPARISON OF PARAMETRIC DUCT-BURNING TURBOFAN AND NON-AFTERBURNING TURBOJET ENGINES IN A MACH 2.7 TRANSPORT

by John B. Whitlow, Jr.
Lewis Research Center
Cleveland, Ohio 44135

March 1975

This information is being published in preliminary form in order to expedite its early release.

ABSTRACT

A parametric study was made of duct-burning turbofan and suppressed dry turbojet engines installed in a supersonic transport. A range of fan pressure ratios was considered for the separate-flow-fan engines. The turbofan engines were studied both with and without jet noise suppressors. Single- as well as dual-stream suppression was considered. Attention was concentrated on designs yielding sideline noises of FAR 36 (108 EPNdB) and below. Trades were made between thrust and wing area for a constant takeoff field length. The turbofans produced lower airplane gross weights than the turbojets at FAR 36 and below. The advantage for the turbofans increased as the sideline noise limit was reduced. Jet noise suppression, especially for the duct stream, was very beneficial for the turbofan engines as long as duct burning was permitted during takeoff. The maximum dry unsuppressed takeoff mode, however, yielded better results at extremely low noise levels. Noise levels as low as FAR 36-11 EPNdB were obtained with a turbofan in this takeoff mode, but at a considerable gross weight penalty relative to the best FAR 36 results.

E-8269

COMPARISON OF PARAMETRIC DUCT-BURNING TURBOFAN AND NONAFTERBURNING TURBOJET ENGINES IN A MACH 2.7 TRANSPORT

by John B. Whitlow, Jr.
Lewis Research Center

SUMMARY

A parametric mission study was made for duct-burning turbofan and suppressed dry turbojet engines installed in a supersonic transport of fixed range and payload. A range of fan pressure ratios from 2.2 to 3.5 was considered for the separate-flow-turbofan engines. The turbojet engines were always equipped with a jet noise suppressor, but the turbofans were considered both with and without suppressors. Single- as well as dual-stream suppression was considered for the turbofan engines. Attention was concentrated on designs yielding sideline noises of FAR 36 (108 EPNdB) and below. Trades were made between thrust and wing area for a constant 10 500-foot (3200-m) FAR takeoff field length. The turbofans produced gross weights as much as 13 percent lower than the 750 000-pound (340 200-kg) turbojet value at the FAR 36 sideline noise level. The advantage for the turbofans increased as the sideline noise limit was reduced. Jet noise suppression, especially for the duct stream, was very beneficial for the turbofan engines as long as duct burning to the limit for uncooled suppressors was permitted during takeoff. The maximum dry unsuppressed takeoff mode, however, yielded better results at extremely low noise levels. Noise levels as low as FAR 36 - 11 EPNdB were obtained with a 2.2 fan pressure ratio engine at maximum dry thrust. A 24-percent increase in gross weight was required, however, for this 11 EPNdB noise reduction, relative to the best duct-burning turbofan results at FAR 36.

E-8269

INTRODUCTION

The parametric mission study being reported here is an outgrowth of recent NASA-Lewis in-house studies of noise-limited turbojet (ref. 1) and duct-burning turbofan (ref. 2) engines installed in Mach 2.7 transports. Although reference 2 largely concerns the benefits that might arise from the use of hydrogen fuel, some results were presented with conventional fuel, for comparison. Unfortunately, the results of the two studies cannot be directly compared because of cycle and mission inconsistencies. For example, tailpipe pressure losses were ignored in reference 1 but included in reference 2. Also, some of the component design efficiencies were different between the two studies when in reality there is no justification for such differences as long as the level of technology is held constant. Similarly, the all-important jet noise suppressor characteristics were different between the two studies.

The present study is an attempt to compare the turbojet and the duct-

burning turbofan engine on a consistent basis. A much broader spectrum of design fan pressure ratio and bypass ratio is included in this study than in reference 2, however, in order to better optimize the duct-burning turbofan cycle over a wider range of sideline noise at FAR 36 and below. These engines were considered over a range of takeoff throttle settings both with and without suppressors. The turbojet part of this study, on the other hand, is much more limited since only one stream is involved in the takeoff noise-against-thrust optimization. Only suppressed turbojets were considered in the present study because reference 1 showed that at the FAR 36 sideline noise level extreme engine oversizing was required for unsuppressed turbojets.

During the same time period that these in-house parametric studies were being made, contracts were let by NASA-Lewis to General Electric and Pratt & Whitney for an "Advanced Supersonic Propulsion System Technology Study." The Phase I results of these contracted studies have already been issued (refs. 3 and 4) and work in the Phase II extensions of these contracts is now in progress. The Phase I contracted work covered unconventional as well as conventional engines and, briefly, the use of liquid hydrogen as an alternative fuel. The two engine types which are the subject of this report were also studied in these contracts. It is difficult, however, to make direct comparisons between the results of the in-house parametric study and the contracted studies because the ground rules are somewhat different (e.g., standard day performance is used in this study whereas standard + 14.4° F (8° C) performance was used in the contracted studies).

Although similarities do exist, the in-house study was for the most part carried on independently of the contracted effort. During the course of the contracts, however, differences would arise in the approaches used by the two contractors to a particular problem which seemingly could be resolved by incorporating both approaches in the in-house parametric study. The most notable example of this occurred in the determination of which exhaust streams to suppress with the duct-burning turbofan engines during takeoff. The approach taken by one contractor was to suppress only the outer stream. The other contractor initially planned to suppress only the inner stream but later decided that both streams ought to be suppressed after determining that duct burning during takeoff could significantly improve the airplane figure of merit. The contractors' decisions as to which streams to suppress were influenced by their choice of cycle design parameters (e.g., fan pressure ratio, bypass ratio, and turbine-inlet temperature). The approach taken in the present study to resolve this stiuation was to examine all possible suppressor modes (i.e., core and duct streams alone, as well as the two combined) over a wide spectrum of cycle design parameters at various levels of takeoff throttle setting. No attempt was made to assess the impact of the additional mechanical complexity of dual-stream retractable suppressors, although weight and thrust penalties were introduced for an additional number of tubes.

Another major difference between the in-house studies and the contracted studies concerns takeoff wing loading. In contracted work re-

ported in references 3 and 4, wing and thrust loading were held fixed for the most part. However, a limited investigation in reference 3 did show some benefit for reduced wing loading at throttle settings giving a sideline noise in the vicinity of FAR 36 (i.e., 108 EPNdB). No attempt was made to optimize wing loading with throttle setting and, hence, sideline noise level. In the present study, however, trade-offs were made between wing and engine size for various takeoff throttle settings at a constant field length. This field length, incidentally, is over 15 percent shorter than that used as the baseline in the Phase I contracted studies. These trade-offs were examined because of the large airflows that are required at lower noise levels with constant thrust. Larger wing planform areas (i.e., lower takeoff wing loadings) reduce the required thrust and thus engine size. Reduction of engine size reduces engine weight at the expense of larger, heavier wings. These trade-offs seemed to be worthy of investigation and were made a part of this study.

ANALYSIS

Mission

The parametric engines of this study were evaluated over a reference Standard Day 4000-nautical-mile (7408-km) mission, the first 600 miles (1111 km) of which were subsonic. Supersonic cruise is at Mach 2.7; subsonic cruise at the beginning of the reference mission is at Mach 0.95. The initial cruise altitude was selected to maximize the quotient of lift-drag ratio divided by specific fuel consumption in a constant Breguet cruise, both subsonically and supersonically. A thrust margin of at least 20 percent was required during climb/acceleration. Selected engines were also evaluated with reduced subsonic cruise legs to determine the influence of this requirement, but the total range, nevertheless, remained fixed. The climb and acceleration flight path, in Mach number and altitude coordinates, is shown in figure 1. When the Mach 0.95 cruise altitude optimizes at a point higher than the 28 000-foot (8534-m) value shown in figure 1 for this speed, acceleration after this segment occurs at a constant altitude until the altitude-Mach number curve shown is intersected. A 250-nautical-mile (463-km) descent from the final Mach 2.7 cruise altitude is included in the basic 4000-mile (7408-km) mission. For the purposes of block time computation, it was assumed that this descent would take 25 minutes.

The total fuel load aboard an airplane includes not only the fuel needed to satisfy the above-stated mission requirements, but also enough to satisfy certain reserve fuel requirements. For this study, the reserve fuel consisted of an additional amount equivalent to: (1) 7 percent of the mission fuel; (2) a 260-nautical-mile (482-km) diversion at Mach 0.95 (at optimum altitude) to an alternate airport; and (3) a 30-minute hold at Mach 0.4 at a 1500-foot (457-m) altitude. These rules are essentially a simplified version of FAR 121.648 proposed by the FAA for supersonic transports.

Airframe

The parametric engines of this study were evaluated by analytically "flying" them in an advanced Mach 2.7 arrow-wing design. Fuselage dimensions were fixed for a constant 234-seat capacity, but wing area was allowed to vary as wing loading was optimized in seeking a minimum gross weight. Engine and wing size tradeoffs were made to minimize takeoff gross weight at any given sideline noise level while retaining a 10 500-foot (3200-m) FAR takeoff field length capability. Wing aspect ratio was held constant as the optimum wing loading was sought. The tail area varied as a fixed fraction of the wing area. The airframe data used in this study is based on a reference arrow-wing design (a refined SCAT 15F-type) supplied by the NASA-Langley Research Center in August, 1972. The reference airplane, a sketch of which is shown in figure 2, has a takeoff gross weight of 750 000 pounds (340 200 kg) and a wing area of 10 000 square feet (929 m^2). The corresponding takeoff wing loading W_g/S is 75 pounds per square foot (366 kg/m^2).

Empty weight. - For the purposes of this study the turbojet engines of the Langley reference airplane were removed and the various parametric engines (including their inlets and nacelles) to be evaluated were substituted. The propulsion system weight (including inlets and nacelles) will be discussed later. Only the weight of the airframe less inlets and nacelles will be discussed at this point. The airframe weight is assumed to consist of two types of components: (1) those whose weights vary with changes in takeoff gross weight and wing loading and (2) those whose weights remain fixed. Into the first category were placed the wing, tail, and landing gear weights. All other component weights (e.g., fuselage, furnishings, hydraulic and electrical systems, electronics, etc.) were assumed to fall into the second, or fixed-weight category.

The wing weight estimate furnished by NASA-Langley for the reference configuration of figure 2 was 80 000 pounds (36 287 kg). An equation was developed, based on empirical data from many airplanes of various types (ref. 5), which permits scaling from the reference weight to a new weight corrected for changes in takeoff gross weight and wing loading. Since the reference gross weight and wing loading were, respectively, 750 000 pounds (340 200 kg) and 75 pounds per square foot (366 kg/m^2), this equation takes the form

$$\left.\begin{aligned} W_{wing} &= 80\ 000\left[\frac{75}{W_g/S} \times \left(\frac{W_g}{750\ 000}\right)^2\right]^{0.64} \quad \text{(lb)} \\ &= 36\ 287\left[\frac{366}{W_g/S} \times \left(\frac{W_g}{340\ 200}\right)^2\right]^{0.64} \quad \text{(kg)} \end{aligned}\right\} \tag{1}$$

for the airplanes in this study. The tail area was assumed to vary in proportion to the wing area and therefore had a weight which varied. This tail weight was related to gross weight and wing loading by the

equation

$$\left.\begin{aligned} W_{tail} &= 0.989 \frac{W_g}{W_g/S} \text{ (lb)} \\ &= 4.82 \frac{W_g}{W_g/S} \text{ (kg)} \end{aligned}\right\} \quad (2)$$

The third item of variable weight in this study was that of the landing gear, which was assumed to be related only to gross weight by the equation

$$W_{\ell g} = 0.0451 \, W_g \quad (3)$$

The total fixed weight for the airframes of this study came to 119 300 pounds (54 114 kg). The airframe weight was obtained by adding this fixed weight to the variable weights computed by equations (1), (2), and (3) with the result that

$$W_{af} = 80\,000\left[\frac{75}{W_g/S} \times \left(\frac{W_g}{750\,000}\right)^2\right]^{0.64} + 0.989 \frac{W_g}{W_g/S} + 0.0451 \, W_g + 119\,300 \text{ (lb)}$$

$$= 36\,287\left[\frac{366}{W_g/S} \times \left(\frac{W_g}{340\,200}\right)^2\right]^{0.64} + 4.82 \frac{W_g}{W_g/S} + 0.0451 \, W_g + 54\,114 \text{ (kg)} \quad (4)$$

To obtain the takeoff gross weight, the above airframe weight must be added to the propulsion system weight, the payload and the fuel load. The propulsion system weight is a variable depending on engine selection. The fuel load varies with the engine selection and is the amount required to provide a range of 4000 nautical miles (7408 km) with enough reserve fuel left over to satisfy the requirements listed previously in the Mission section. The payload, however, is fixed and represents at 48 906 pounds (22 183 kg) the weight of 234 passengers and their baggage.

Aerodynamics. - Drag polars for the reference 10 000-square-foot-(929-m^2) wing airplane were supplied by NASA Langley at selected Mach numbers. In some cases the altitude corresponding to each Mach number was slightly different from that displayed in figure 1. Adjustments were then made to the polars to make them correspond to the altitude-Mach number placard of figure 1. (Reynolds number and compressibility effects vary somewhat with altitude to change the skin friction coefficients.) The polars were parabolic and so could be expressed mathematically in the form

$$C_D = C_{D_{min}} + \left[\frac{C_{D_i}}{(C_L - C_{L_O})^2}\right](C_L - C_{L_O})^2 \qquad (5)$$

Schedules of $C_{D_{min}}$, $C_{D_i}/(C_L - C_{L_O})^2$, and C_{L_O} against Mach number are shown in figure 3 for the reference airframe having inlets and nacelles sized for 633-pound-per-second (287-kg/sec) turbojets. These schedules describe the polars which have been corrected to the altitude-Mach number placard of figure 1. The high values of $C_{D_{min}}$ below Mach 0.4 reflect the increased drag incurred by the high flap settings used in takeoff.

The $C_{D_{min}}$ schedule of figure 3 is for the reference airframe having a wing planform area of 10 000 square feet (920 m^2). In this study, the gross weight and wing loading, and therefore the wing size, will change while the fuselage dimensions are fixed. The engine pod dimensions also will change. Since each component is being scaled up or down more or less independently of the other, the $C_{D_{min}}$ schedule should vary from that of the reference airplane. Drag buildup curves showing the amount of drag accounted for by each component are needed before the effect of relative area changes can be determined. Unfortunately, these were not readily available. Drag buildup assumptions, nevertheless, were made for this part of the study, based on previous data for other configurations.

The airframe component areas and dimensions for the reference airplane were estimated as a first step in the synthesis of a drag buildup procedure. The airframe was broken down into a set of components: wing, body, vertical tail, horizontal tail, and nacelles. Total minimum drag from the reference airplane was assumed to be composed of the sum of the friction and pressure, or wave, drags of these components.

The component skin friction coefficients were calculated by means of the Prandtl-Schlichting equation

$$C_{fic_{component}} = \frac{0.455}{(\log_{10} Re_{component})^{2.58}} \qquad (6)$$

This equation gives the skin friction coefficient for incompressible turbulent flow over one surface of a flat plate. These coefficients were then corrected for compressibility effects by a correction factor which was a strong function of Mach number and a weak function of altitude. These correction factors are based on empirical turbulent flow flat plate data (e.g., ref. 6) which vary with Reynolds number and Mach number. The total airplane friction drag coefficient, based on wing planform area, was obtained by correcting the component skin friction coefficients to a common reference wing area and adding, as follows:

$$C_{D_{f_{total}}} = 2\left(C_{f_{wing}} + C_{f_{vt}} \times \frac{S_{vt}}{S_{wing}} + C_{f_{ht}} \times \frac{S_{ht}}{S_{wing}}\right) + C_{f_{body}} \times \frac{S_{body}}{S_{wing}} + 4C_{f_{nac}} \times \frac{S_{nac}}{S_{wing}} \quad (7)$$

The wing, vertical tail, and horizontal tail skin friction coefficients in this equation are doubled to account for both surfaces of these components. The nacelle coefficients are multiplied by four to account for the fact that a four-engine configuration is being considered.

The pressure drag coefficients of each of the various components based on a representative component area are corrected to the wing planform area and added, as follows:

$$C_{D_{p_{total}}} = C_{D_{p_{wing}}} + C_{D_{p_{vt}}} \times \frac{S_{vt}}{S_{wing}} + C_{D_{p_{ht}}} \times \frac{S_{ht}}{S_{wing}} + C_{D_{p_{body}}} \times \frac{A_{body}}{S_{wing}} \quad (8)$$

The nacelle pressure drag does not appear as a separate term in this equation but is combined with that of the wing, since it is difficult to isolate the two in a highly integrated configuration. The body and tail pressure drag coefficients based on their representative component areas are assumed to be scheduled with Mach number in the same manner as representative empirical data for these types of components in other airplanes. The wing pressure drag coefficient was varied in an iterative calculation at each Mach number until the total minimum drag coefficient obtained by adding equations (7) and (8) agreed with the reference $C_{D_{min}}$ (fig. 3).

In the parabolic drag polar equation (eq. (5)), both the induced drag term within brackets and C_{L_0} were assumed to have a schedule against Mach number (top two curves of fig. 3) that did not change with variations of the relative component dimensions. The $C_{D_{min}}$ term will, however, vary as the body-to-wing area ratios in equations (7) and (8) change. (The area ratios between the tail components and the wing remain constant in this study.) In addition, the skin friction coefficients of the wing, tail, body, and nacelle components change because of changes in the characteristic length in the Reynolds number term of equation (6). The component pressure drag coefficients based on their own representative areas (eq. (8)) are assumed to have a fixed schedule with Mach number. Typical variations in $C_{D_{min}}$ resulting from this type of analysis are shown in figure 4 for two optimized study airplanes. The reference $C_{D_{min}}$ schedule (fig. 3) from which these adjustments were made is also shown.

The two optimized airplanes are representative of those using unsup-

pressed duct-burning turbofans and suppressed dry turbojets constrained to the FAR 36 (108 EPNdB) sideline noise condition. The enlarged wing planform of the optimized turbofan configuration (the larger of these two optimized planforms) is compared to the reference configuration in figure 5. Such a configurational change produces an airplane layout which is probably similar enough to the reference for the incremental drag estimation procedure outlined here to be valid. The accuracy of the procedure should deteriorate, however, as the noise level is reduced and the trade is toward still larger wings. This is especially true for the unsuppressed engines. The optimum airplanes which result with suppressed duct-burning turbofans will be much closer to the reference. At the FAR 36 sideline condition, for example, the optimum suppressed turbofan configuration will be almost identical to the reference airplane.

The $C_{D_{min}}$ schedules shown for the optimized airplane examples in figure 4 are lower than the reference schedule because the wing planform areas are larger. The actual drag (as opposed to the drag coefficient) at any given C_L will be higher for the optimized airplanes because the decrement in $C_{D_{min}}$ is less than the increment in wing area. The C_L will be less, however, in the optimized cases because they have a lower wing loading. The induced drag will thus be a smaller fraction of the total drag than in the reference case.

The C_L that can be developed at the point of lift-off (at approximately Mach 0.3) is of prime importance in determining the engine thrust requirement for a fixed field length, wing area, and takeoff gross weight. It is limited by the angle of attack that can be pulled without dragging the tail on the runway. A lift-off C_L of 0.55 was used for the airplanes of this study.

Engines

Both dry turbojet and duct-burning turbofan engines were studied. Design component characteristics, as shown in table I, were selected for a maximum consistency of technology between the two engine types for this comparative study. Only one turbojet cycle was studied. Varying amounts of throttling were considered during takeoff for these suppressed engines to obtain gross weights for a spectrum of sideline noise values. A similar evaluation was made for each of four different duct-burning turbofan cycles. The matrix of data generated for the turbofan engines, however, was much greater because, for each cycle, takeoffs both with and without duct burning and with and without suppression were considered. Single-stream and dual-stream jet suppression were compared for the separate-flow-fan engines. Fan pressure ratios from 2.2 up to 3.5 were studied. Bypass ratio was selected at each FPR by a quasi-optimization procedure which considered sideline noise and takeoff thrust-to-engine weight ratio. An overall compressor pressure ratio of 10 was selected for all the engines, including the dry turbojet. The results of reference 7 indicated that this value was about optimum in the presence of a noise constraint

for the high turbine temperature selected for this study.

A design turbine rotor-inlet temperature of 2725° F (1496° C) was selected as being the maximum allowable for a reasonable cooling bleed flow and metal temperature in the high-pressure rotor with advanced full-coverage film cooling. No perturbations were made to this design parameter because previous results (ref. 2) showed this temperature was an optimum when noise was constrained to FAR 36 levels, even though no turbine efficiency penalty was assessed for the higher bleed flows required at higher temperatures.

With the turbofan engines, the duct burner temperature was held to a maximum of 1600° F (871° C) in takeoff when duct jet suppressors were used in order to stay below the suppressor materials technology limit. The duct burner was turned off after takeoff and relit just prior to Mach 1. Duct burning was continued at 2300° F (1260° C) until the Mach 2.7 cruise condition was reached. At this point, the duct-burner temperature was reduced to match thrust to drag.

With the turbojet engines, the same 1600° F (871° C) suppressor materials technology limit would apply at takeoff. To obtain a sideline noise level of 108 EPNdB (i.e., FAR 36), it was necessary to throttle these engines back so that the exhaust gas temperature was 1500° to 1600° F (815° to 871° C) when advanced technology multitube suppressors were used. Therefore, at the noise levels of interest at FAR 36 and below, there was no suppressor materials problem.

The suppressors used for both the turbojet and turbofan engines of this study were assumed to follow the schedule of suppression against fully expanded exhaust velocity shown in figure 6. An additional gross thrust loss of 7.5 percent was assumed for the suppressors when deployed, regardless of exhaust velocity. The suppressor technology represented by these characteristics is more advanced than has been demonstrated to date in flight-weight hardware but is considered possible for airplanes being developed for initial service in the mid-1980's. A weight penalty, to be discussed later, was assessed for suppressor-equipped engines.

Component matching and mode of operation. - Engine component flow areas are sized for the pressures, flow rates, shaft speeds, and efficiencies chosen for a certain design-point condition. In this study, the sea-level-static condition in a 1962 U.S. Standard Atmosphere was selected as the engine design point. With the various flow areas fixed by the design-point sizing criteria, pressure ratios, flow rates, shaft speeds, and component efficiencies will change as Mach number, altitude, and/or throttle setting are changed. These changes occur when the components rematch to satisfy conditions of flow continuity and power balance that must exist between the driven fan and compressor and their driving turbines.

Rematching off-design can be altered to some extent by using variable-area components to obtain a more favorable result. In these

studies, the primary exhaust nozzle throat area was adjusted in takeoff to obtain the best possible thrust against jet noise trade with a given design. In general, this involved opening the throat area to allow more flow at a reduced exit velocity. Several turbine-rotor-inlet temperatures at and below the 2725° F (1496° C) design value were considered for each engine in this takeoff optimization.

The primary exhaust nozzle throat area was also manipulated in subsonic cruise to retain full-throttle airflow at part-throttle conditions to minimize spillage drag. In supersonic cruise, the same procedure was followed with the dry turbojets at the required reduced turbine-inlet-temperature condition. Reduced thrust was obtained in the duct-burning turbofan engines, however, by reducing only the duct-burner temperature from its maximum supersonic climb value of 2300° F (1260° C). Hence, it was unnecessary to adjust the primary nozzle area for supersonic cruise, but the duct-stream nozzle throat area was allowed to float to avoid rematching the engine as the temperature of that stream was changed. Since there was no rematch for reduced thrust, there was no airflow change and thus no spillage increment. In no case was any nozzle throat area ever increased by more than 50 percent from its design value in order to provide some degree of mechanical realism.

Design and off-design performance calculations for the single-spool turbojets and the two-spool duct-burning turbofans of this study were made with the GENENG computer program (ref. 8). Fan, compressor, and both high- and low-pressure turbine maps for each type of engine were stored in the program. The maps are required for use in the off-design calculations. They are nondimensionalized in the computer program to facilitate scaling as design parameters are changed.

Turbine cooling. - Compressor discharge air was bled around the primary combustor to cool the turbine. Bleed air requirements for blade temperatures of 1750° F (954° C) and vane temperatures of 1850° F (1010° C) were calculated by using the full-coverage-film-cooling curve of reference 9. The single high-pressure turbine of the turbojet was assumed to have two stages. The duct-burning turbofan engines all had a single-stage high-pressure turbine and either three or four low-pressure stages, depending on the work extraction which was a function of fan pressure ratio and bypass ratio. Bleed used for cooling the high-pressure turbine of the turbofan engines was assumed to be available for work in the low-pressure turbine stages. No work was recovered from any of the air used to cool the low-pressure turbine. Likewise, there was no bleed-air turbine work recovery in the single-spool turbojet engines.

The cooling requirement is most severe at the Mach 2.7 condition because the cooling air coming from the compressor discharge is about 1020° F (549° C) for all the study engines (since they all have an overall compressor pressure ratio of 10). According to reference 10, a stage bleed flow of 3 percent is in the middle of the usable range. Accordingly, this value was chosen for the first stage turbine rotor, exclusive of wall

and shroud considerations. A cooling effectiveness of 0.565 was obtained for this amount of bleed from the curve of reference 9 for the first stage rotor. The definition of cooling effectiveness yields a rotor-inlet temperature of 2725° F (1496° C) when the metal temperature is 1750° F (954° C) and the coolant temperature is 1020° F (549° C). Bleed requirements for each succeeding stage (both stator and rotor) were calculated in a similar manner. The stage cooling flow computed by this method was multiplied by 1.33 to account for cooling the shroud and wall in addition to the blade or vane. The total cycle chargeable cooling flows thus obtained were typically about 10 percent of the compressor discharge air (see table I). (High-pressure turbine stator cooling is not cycle-chargeable.)

Weight. - Bare engine weights were obtained by the correlation technique of reference 11. The year 1974 was substituted into the reference 11 formulas to establish a level of weight technology for these study engines. Reference 11 was published in 1970 and made projections of engine weight reduction into the future. So far, these projections have been overly optimistic and a so-called "1974" level of technology is representative of advanced weight technology for new engines presently undergoing preliminary design. Reference 11 provides an estimated weight minus duct burners, exhaust nozzle/suppressor/reverser, and accessories. To obtain the propulsion system weight, these components as well as inlet and nacelle weight plus other installation items must be added to the bare weight calculated by this procedure. The propulsion system weight total for all four engines, when added to the airframe weight calculated from equation (4), gives the operating empty weight (OEW).

Figure 7 shows how the bare weight calculated by the method of reference 11 varies with bypass ratio for a single engine having a sea-level-static corrected airflow of 1000 pounds per second (454 kg/sec). An overall compressor pressure ratio of 10 and a turbine temperature of 2725° F (1496° C) were used in these calculations. Fan pressure ratio effects are not included in the reference 11 analysis. They were believed to produce only second order effects.

Empirical data for nozzle weights of supersonic engines is difficult to obtain because usually only the engine weight with nozzle included is quoted in brochures. Most existing supersonic engine data is for military engines where the high-supersonic requirement is merely for short-term dash. Military engines are likely to have their high-supersonic performance sacrificed somewhat in favor of reduced weight. Such trades are not likely to be favorable for a long-range supersonic cruise vehicle like a Mach 2.7 transport, where good supersonic cruise performance is of prime importance. Also, military engine design life considerations are not as demanding as those for commercial engines. Furthermore, military engines require no suppressors and often no thrust reversers either. These considerations tend to make the exhaust system for a supersonic cruise commercial engine heavier than those in typical military fighter and bomber installations. The data base available for exhaust system

weight estimation, then, is limited for the supersonic cruise application of this study and is therefore subject to a higher degree of uncertainty than weight data used for the bare engine.

The weight used for the nozzle/reverser/suppressor assembly for the turbojet engine in this study was 10 700 pounds (4853 kg) for an arbitrarily selected 1000-pound-per-second (454-kg/sec) reference size. This high weight reflects the temperature and pressure environment in which the assembly must be operated plus the complexity involved in incorporating all the variable geometry features required to obtain satisfactory nozzle performance over a wide range of operating conditions. An added complexity is the retractable multitube jet noise suppressor.

To the bare weight of all the turbofan engines obtained from figure 7 was added 500 pounds (228 kg) to account for the duct burners and their related hardware. Then 5650 pounds (2563 kg) were added for the nozzle/reverser assembly. If only a single-stream suppressor was used, another 1000 pounds (454 kg) was added. (This increment was the same whether the suppressor was used on the duct stream or the core stream.) When both streams were suppressed, the increment for suppressor weight was 1700 pounds (771 kg). All of these nozzle/reverser and suppressor weight increments are based on the reference engine size of 1000 pounds per second (454 kg/sec).

The weight of the inlet plus nacelle was assumed to be the same for both turbojet and turbofan engines with the same design airflow. This weight was scaled up to the 1000-pound-per-second (454-kg/sec) reference engine size from Boeing data for the GE4/J5P installation in the 2707-300 SST. This scaling, combined with a 10-percent reduction for technology advancements, produced a weight of 5375 pounds (2438 kg) per engine installation. A further installation penalty of 1455 pounds (660 kg) per engine was added to account for miscellaneous installation items. This, too, represents a 10-percent reduction from that used in the 2707-300 weight statement to account for possible technological advancements. Ten percent, incidentally, is the weight reduction postulated by the Gerend bare engine weight estimating technique (ref. 11) for a two-year advance of technology.

To obtain a reference propulsion system weight for inclusion in the airplane weight statement, the weight of the bare engine, duct burner (if applicable), nozzle/reverser, suppressor (if any), inlet/nacelle, and miscellaneous installation items must be summed and multiplied by the number of engines (four). This weight must then be scaled if an engine size other than the 1000-pound-per-second (454-kg/sec) reference is to be used in the airplane. The scaled propulsion system weight is given by the equation

$$W_{prop} = W_{prop,ref} \times \left(\frac{\dot{W}_{2c}}{1000}\right)^{1.2} \quad \text{(lb)}$$

$$= W_{prop,ref} \times \left(\frac{\dot{W}_{2c}}{454}\right)^{1.2} \quad \text{(kg)} \qquad (9)$$

Sizing. - The engine size (i.e., design airflow) was selected to give sufficient thrust for a FAR takeoff field length of 10 500 feet (3200 m). Designing for such a field length will allow operation from most of the world's principal airports. The thrust-to-gross-weight ratio required to meet this field length criterion should also be sufficient to provide some margin on community fly-over noise at 3.5 miles (6.5 km) from brake release, a noise measuring point stipulated in FAR 36. The airplane altitude and Mach number at the 3.5-mile (6.5-km) point should be high enough so that the noise under the flight path after power cut-back for minimum climb gradient is several EPNdB less than the sideline noise. Sideline noise (as defined by FAR 36) is the maximum noise incurred at takeoff or in the initial climb-out measured on a line parallel to the runway centerline but 0.35 nautical mile (648 m) to the side. The maximum is expected to occur after lift-off at an altitude of 800 feet (244 m) or more when no further benefit from extra ground attenuation and fuselage-masking of half the engines is realized.

The takeoff thrust-to-gross-weight ratio required for lift-off in some fixed distance can be shown theoretically to be proportional to wing loading divided by lift coefficient at lift-off if second order effects like thrust-drag ratio are ignored (ref. 12). The FAR takeoff field length, which includes a safety margin for an engine-out as well as clearance of a 35-foot (11-m) obstacle at the end of the runway, becomes a rather complicated calculation. It is best handled for the purposes of this study on an empirical basis. For four-engine transports of the type considered herein with a C_L of 0.55 at lift-off, the thrust-weight ratio needed for a 10 500-foot (3200-m) FAR field length was estimated as

$$(F_n/W_g)_{M=0.15} = 0.00439(W_g/S) \quad \text{(lb/lb)}$$

$$= 0.000900(W_g/S) \quad \text{(N/N or kg/kg)} \qquad (10)$$

The subscript $M = 0.15$ in this equation indicates that the calculated F_n/W_g is an average between the brake release static condition and the lift-off condition at approximately Mach 0.3. The average was used to allow for the fact that the various parametric engines have different thrust-against-speed lapse rates.

The noise on the FAR 36-designated sideline varies alongside the runway and initial flight path until it reaches a peak sometime before the power cut-back for the community noise measurement at 3.5 miles (6.5 km). No effort has been made in this study to schedule takeoff thrust for a constant sideline noise. The throttle setting was fixed

during the entire takeoff procedure.

Jet noise calculations. - The only noise calculations made in this study were for the maximum sideline noise. No extra ground attenuation or fuselage engine-masking were assumed. Sideline noise is believed to be the dominant of those considered in FAR 36, at least in this application where such high thrust-weight ratios are required at takeoff (see eq. (10)). Furthermore, sideline noise is easier to calculate than the 3.5-mile (6.5-km) community noise since no trajectory optimization or throttle adjustments are involved. In the sideline calculation, it is not known at exactly what altitude the maximum noise occurs. In these calculations, that altitude was assumed to be at 800 feet (244 m), but a 25 percent error in this estimate (200 ft or 61 m) will produce only about a 3-percent difference in the sideline-to-airplane distance (about 70 ft or 21 m). It is this latter distance which enters into the noise calculation.

The selection of the parametric engine designs and the optimization of their takeoff throttle setting and exhaust nozzle adjustment were based on minimizing the sideline jet noise as calculated by standard SAE techniques (refs. 13 and 14). These techniques are simplified and approximate, but the benefit of further refinement is questionable in view of the tentative nature of much of the empirical data available. For example, there is reason to believe that some benefit from coannular exhaust streams (as in the duct-burning turbofans of this study) will occur. The SAE technique, however, does not consider any such benefit. The two streams are assumed to generate noise independently of each other with the combined noise being the result of adding antilogarithmically the noise of the two streams. In the calculation of each stream noise, the shear velocity is considered to be the fully expanded jet velocity relative to the free stream. This seems to be a conservative approach, especially for the core stream, which is shielded from the free stream by the outer (duct) stream. The empirical coannular data on which more elaborate turbofan jet noise calculation techniques are based (e.g., ref. 15) consists almost entirely of cases in which the core velocity is higher than the velocity of the outer stream. Many cases are considered in this study in which the situation is just the opposite - that is, the outer stream velocity is higher than that of the core stream. This is especially true for cases where the engine is optimized to use a duct stream suppressor with an unsuppressed core stream. These more refined calculation techniques, although newer than the SAE method used in this study, are not justified for this type of study because their empirical correction factors for coannular exhausts would have to be extrapolated into a region of jet velocity ratio far beyond the data base.

In the sideline noise procedure used in this study, the fully expanded jet velocities used to compute the sound pressure levels were reduced by the amount of the airplane's forward velocity, as per reference 13. This relative velocity credit is perhaps only partially obtained in actuality. In this respect, the SAE noise procedure used herein

is optimistic and estimates noise levels which are perhaps too low. Modification of the relative velocity term is one of the revisions being considered by the SAE's Committee A-21 in up-dating the jet noise calculation procedure.

FAR 36 sets noise limits in terms of effective perceived noise level (EPNdB) whereas the SAE procedure used here gives results in perceived noise level (PNdB). The difference is that effective perceived noise has a duration correction which is added to the perceived noise level to account for the length of time the observer hears the noise. This correction is based on the integrated time history of the perceived noise level at the observer's location, with time beginning and ending when perceived noise level is 10 dB below the peak. The SAE method used here calculated only this peak noise which is assumed to occur at 45° to the exhaust jet axis (an assumption which is strictly valid only for a standard circular nozzle). The intensity of perceived noise over the directionality spectrum must be known (not just the 45° peak value) to compute this correction factor. Unfortunately, the SAE method gives no information about directionality. The impact of the duration correction factor was studied at the sideline condition by using the computerized Boeing/NASA-Ames noise program (ref. 15) to simulate the jet noise from representative turbojet and coannular-exhaust turbofan engines at various throttle settings. The correction factors varied with engine type and throttle setting within a band of ±1 dB. Based on these observations, it seemed that little would be gained in these sideline noise calculations by the added complication of actually converting from perceived to effective perceived noise level. Instead, the simplifying assumption was made that sideline noise in EPNdB would be equal to the PNdB values as calculated by the SAE method.

Installation. - An inlet pressure recovery schedule similar to that of the Boeing 2707-300 (ref. 16) was used in these engine performance calculations. Variable inlet geometry was assumed to provide external compression at speeds up to Mach 1.6 with the centerbody fully extended. Beyond Mach 1.6 the centerbody was fully retracted for external-internal compression. At Mach 2.7, there was no spillage or bypass; inlet drag consisted entirely of that due to dumping boundary layer bleed air. During Mach 2.7 cruise, engine airflow was unchanged from its full-throttle value. The inlet drag during cruise, therefore, was independent of power setting. During full-power supersonic climb and acceleration, spillage was the dominant component of inlet drag up to about Mach 2.2. No secondary airflow from the inlet was assumed for the exhaust nozzles.

The exhaust nozzle gross thrust coefficient for each nozzle (including the dual separate-flow nozzles of the turbofan engines) was fixed at 0.98 for all flight conditions except during the Mach 0.95 cruise leg and the reserve cruise to alternate. At these conditions, the thrust coefficient was reduced to 0.90 to account for boattail drag penalties likely to prevail in the transonic region at reduced thrust. As mentioned previously, when suppressors were deployed at takeoff, an additional 7.5-percent gross thrust penalty was charged after the application of the 0.98

nozzle gross thrust coefficient.

RESULTS AND DISCUSSION

Selection of Turbofan Bypass Ratio

Design fan pressure ratios of 3.5, 3.0, 2.5, and 2.2 were selected for study. Design bypass ratio was selected without an actual optimization after considering its impact on the lift-off thrust-to-podded-engine-weight ratio and sideline noise from four 1000-pound-per-second (454-kg/sec) engines. Thrust-to-weight ratio and maximum sideline noise after lift-off are plotted against sea-level-static design bypass ratio in figure 8(a) to (d) for a maximum dry (unaugmented) takeoff. The bypass ratio selection at each fan pressure ratio is shown in the figures. Unless otherwise indicated, no jet noise suppression was used. In each case shown, the thrust-to-weight ratio declines linearly as BPR is increased. The total jet noise simultaneously declines at a rapid rate, eventually flattening and becoming tangent to the duct noise floor.

An FPR of 3.5 was the highest chosen because the unsuppressed dry duct noise is at approximately the FAR 36 noise level (bottom of fig. 8(a)). A total noise of 108 EPNdB can never be obtained without suppression by increasing BPR, however, because the duct noise floor at the lift-off condition rises above FAR 36. Since there was no hope of obtaining FAR 36 without suppression (with the reference size engines, at least), a bypass ratio was selected to provide the core stream with an exit velocity of 2500 feet per second (762 m/sec) - the optimum for maximum suppression (see suppressor characteristic curve, fig. 6). It is seen from the top part of figure 8(a) that, even at this condition (BPR = 1.23) with core suppression, the sideline noise is slightly above FAR 36. The same noise level without a core suppressor would be obtained at a BPR of 2.2. The thrust-to-weight ratio obtained at the lower bypass ratio is 4.5 percent higher, however, even with the weight and thrust penalties of the suppressor. Hence, if the engines are sized by takeoff thrust, there will be an engine weight saving with the suppressed core when compared to the higher BPR unsuppressed case at the same noise level. The lower BPR case will also very likely give a better supersonic cruise sfc. As can be seen in the top part of figure 8(a), the suppressed noise level will never be brought all the way down to FAR 36 by increasing the bypass ratio. The thrust-to-weight penalty does not appear to be worth the small further noise reduction possible by raising the BPR from the value selected with a suppressed core.

A bypass ratio of 2.0 was selected for the FPR of 3.0 because this was the reference engine for a recent previous study (ref. 2) from which much performance data were already available. The noise and thrust-weight data for a maximum dry unsuppressed takeoff is shown in figure 8(b) for a fan pressure ratio of 3.0. The duct noise floor is about 4 EPNdB lower than for the FPR = 3.5 engine. The unsuppressed core noise can, therefore, be greater than the duct noise and still have a total noise at

or below FAR 36. The BPR = 2.0 selection produced a total sideline noise about 5 EPNdB above FAR 36. The noise could have been brought down to FAR 36 by raising the design BPR to 2.4 at the expense of reducing F_n/W_{eng} by about 5 percent. A further optimization of the takeoff operating mode, to be examined later in greater detail, shows that opening the core nozzle throat area by 30 percent from its design value reduces the total sideline jet noise to about FAR 36 at BPR = 2.0 while decreasing F_n/W_{eng} only slightly (as shown by the truncated curves at BPR = 2.0 in fig. 8(b)). Both the fan and compressor spools overspeed somewhat when the core nozzle throat is opened. This causes more energy to be taken out of the turbines, thereby deenergizing the core stream and reducing its noise level. The duct noise is raised about 2 EPNdB by the 30-percent increase in area because overspeeding the fan drives its pressure ratio upward. The noise levels of the core and duct streams are more nearly equal at BPR = 2.0 after this adjustment to the core nozzle throat area. Manipulation of this area results in a higher F_n/W_{eng} than was possible by increasing the design BPR to 2.4 to obtain FAR 36. No engine weight penalty was assessed, however, for allowing the engine to overspeed.

The main consideration in the BPR selection for the FPR = 2.5 engine (fig. 8(c)) was to raise the bypass to the maximum possible before the total noise curve flattens out as it approaches the duct noise floor. A bypass ratio of 3.21 was selected. A sideline noise level at about FAR 36 - 6 EPNdB was obtained. A further increase in BPR would have penalized F_n/W_{eng} even more without much additional noise reduction. As with all other turbofan cycles selected in this study, nozzle throat area will be varied during takeoff to rematch the components for the best noise-thrust relation.

The same philosophy that was adopted in selecting BPR at FPR = 2.5 was again used at FPR = 2.2 (fig. 8(d)). A design BPR of 4.18 was chosen for greatest possible noise reduction without unduly compromising F_n/W_{eng}. A sideline noise level of FAR 36 - 11 EPNdB was obtained for the reference 1000-pound-per-second (454-kg/sec) engines.

The lift-off F_n/W_{eng} for each selected BPR steadily erodes as design FPR decreases, as can be seen by progression sequentially from figure 8(a) to (d). This means that the engine size must increase as design FPR decreases (at the selected BPR's) if a constant lift-off thrust is to be obtained at the maximum unaugmented thrust setting. A plot correlating the design FPR's with the BPR's used for this study is shown in figure 9. The circled points representing the engine design parameters chosen for this study are connected by broken straight lines to indicate that no precise or analytical relation is being shown. The BPR selection process just discussed was somewhat arbitrary and there is some latitude in the selection of a satisfactory bypass ratio for each FPR. Despite the lack of precision in the BPR selection process, the trend should always be for BPR to increase as FPR decreases in order to achieve a total jet noise which approaches the duct noise floor. There is a band of BPR's at each FPR that could provide acceptable noise and F_n/W_{eng} trades

with the proper manipulation of the core nozzle throat area at takeoff.

Comparison of Turbojet and Turbofan Cruise Performance

The supersonic cruise installed performance curves are shown in figure 10(a) for each of the four selected duct-burning turbofan cycles as well as the dry turbojet. Specific fuel consumption is plotted against net thrust from the maximum dry setting to the maximum duct-burning setting (duct temperature at 2300° F or 1260° C) for the turbofan engines. The turbine rotor-inlet temperature is constant at its design value of 2725° F (1496° C) for this range of thrust settings. With the dry turbojet engine, however, the design turbine rotor-inlet temperature of 2725° F (1496° C) occurs only at the circled point at the right-hand end of the curve. Thrust reductions from this maximum were accomplished by turbine temperature reductions with constant airflow. All the data in figure 10(a) are for engines of the reference 1000-pound-per-second (454-kg/sec) design airflow.

After properly sizing the engines for adequate takeoff thrust at the various sideline noise levels and optimizing the cruise altitude, the required cruise thrust usually occurs somewhere near the minimum sfc on the engine throttle curves. The throttle curves of figure 10(a) will be shifted horizontally as altitude and engine size are changed, but the sfc corresponding to a particular throttle setting will not change. The lowest sfc minimum occurs with the turbojet. The turbofan engines have their throttle curves grouped at sfc's somewhat higher than the turbojet engine in the region of the minima for these curves. The minimum sfc on each curve increases as the design FPR decreases and the corresponding selected BPR's increase. The minimum of each turbofan curve occurs at a duct temperature of 1100° to 1250° F (593° to 676° C). The minimum sfc on the turbojet curve occurs over a turbine-rotor-inlet-temperature range of 2000° to 2300° F (1093° to 1260° C).

The subsonic cruise installed performance for the same group of engines is shown in figure 10(b). The sfc's should again be compared among cycles in the vicinity of the bucket of each throttle curve. Adjustments made to the cruise altitude to maximize the quotient of L/D divided by sfc tend to cause the required thrust to be near the minima of these curves.

The circled points on the turbofan throttle curves (fig. 10(b)) represent the maximum dry (unaugmented) throttle settings. The corresponding point on the turbojet curve occurs off the thrust scale of the figure to the right. The amount of throttle cut-back required for minimum sfc on the turbofan curves decreases as design FPR is decreased and the corresponding selected BPR increases.

The discontinuity in the two turbofan curves with the highest FPR indicates the abrupt cut-off of turbine cooling bleed when the turbine rotor-inlet temperature is reduced below a certain level. No turbine

cooling bleed was used at rotor-inlet temperatures at or below 1750° F (954° C) because this was the temperature to which the rotor blades were to be cooled at the most critical cooling condition (Mach 2.7 at design rotor-inlet temperature). For the lower design FPR cases (i.e., FPR = 2.5 and 2.2), no cut-off of turbine cooling bleed is shown because higher throttle settings are needed to obtain the required thrust. There is no turbine cooling bleed anywhere on the part of the turbojet throttle curve shown in figure 10(b) since the rotor-inlet temperature is below 1750° F (954° C) in this region. The discontinuity occurs off the right-hand end of the figure.

The best subsonic cruise performance is likely to be obtained with one of the higher FPR turbofans which can take advantage of the turbine cooling bleed cut-off at low throttle settings. The turbofans with design FPR's of 2.5 and 2.2 will be worse because of their need for turbine cooling at the required higher throttle settings. The FPR = 2.2 case, especially, may need a small amount of duct-burning to provide sufficient cruise thrust. If this is the case, its sfc will be worse than that of even the throttled turbojet.

The gain to be obtained by the cut-off of bleed at low power settings may be illusory in actual practice, but theoretically it is possible and seems to be worthy of trying to use. In actual practice, however, valving would have to be introduced to the bleed system at some weight penalty and turbine efficiency might suffer if the bleed flow were suddenly cut off in blades designed for bleed. Neither of these factors was considered in the optimistic approach taken here.

Optimization of Exhaust Nozzle Throat Area During Takeoff

As was mentioned previously in connection with figure 8(b), a more favorable relation between noise and thrust can sometimes be obtained by adjusting the core nozzle throat area to rematch the engine components during takeoff. Since figure 8(b) concerns the FPR = 3.0 cases and how the design BPR of 2.0 was selected, this particular engine will be examined here in greater detail. As was the case in the previous discussion, the engine size will be fixed at a reference value of 1000 pounds per second (454 kg/sec).

Figure 11(a) shows how the manipulation of the nozzle throat area of the fixed FPR = 3.0 (BPR = 2.0) engine design (unsuppressed) affects the lift-off thrust per engine and the maximum sideline noise of four engines. Take, for instance, the curve representing different throat areas at the maximum dry takeoff setting. At the design throat area, represented by a circled point, sideline noise is shown to be 113.3 EPNdB at a thrust of 44 200 pounds (196 610 N). Increasing the throat area until it is 30 percent over design overspeeds the engine somewhat, but reduces the noise level to 108.6 EPNdB with no reduction in thrust. At some power settings (e.g., at 200° F (111° C) below design turbine temperature with no duct burning) the thrust actually increases as the throat area is increased to

seek a noise reduction. Several different power settings are shown in figure 11(a) all the way up to a duct temperature of 1600° F (871° C) with design turbine rotor-inlet temperature. An envelope tangent to all these curves was constructed to show the locus of a curve of maximum thrust against sideline noise for this engine. Tick marks on the envelope curve at the points of tangency show the optimum actual-to-design nozzle throat area at selected power settings. Power settings in which the core was throttled with duct burning were also examined, but their best points fell to the right of the envelope and are not shown.

Figure 11(b) shows a similar plot for the same engine with a duct suppressor added. The thrust values shown reflect the 7.5-percent loss in duct gross thrust charged to the suppressor. With the duct suppressed and the core unthrottled, the core is clearly the dominant noise source at the design nozzle throat area. As the core throat was opened to its maximum allowable of 50 percent over design, reductions were still being obtained in noise with only moderate thrust penalties at design turbine temperature. At a turbine temperature 400° F (222° C) below design, a 40-percent increase in nozzle throat area appeared to be optimum in the absence of duct burning. The envelope curve, representing the best takeoff performance that can be achieved, has been drawn through the points representing a 50-percent nozzle throat area increase for all the power settings with design turbine temperature all the way up to the maximum duct temperature of 1600° F (871° C). With the core throttled with duct burning, curves tangent to the envelope were generated. The points of tangency occur at less than the maximum allowable increase in throat area for these cases. A comparison of the envelope curves between figures 11(a) and (b) shows that a considerable increase in thrust can be obtained at a given noise level by using a duct suppressor. This is especially true as noise level is allowed to increase into the region above 104 EPNdB, where the effectiveness of the duct suppressor improves as the amount of duct-burning increases. The improved thrust at any given noise level with duct suppressors can later be translated into a smaller engine size requirement. A gross weight reduction is not guaranteed, however, because the weight saving of the reduced engine size will have to be traded against the added weight of the suppressor as well as a possible increase in fuel consumption.

Figure 11(c) shows a similar plot where both duct and core suppressors have been added. The thrust values shown reflect the 7.5-percent loss in total gross thrust caused by the addition of suppressors to both streams. With duct burning, the design nozzle throat area appears to be optimum. Without duct burning, the optimum thrust and noise relation is obtained with a 20-percent increase in the core nozzle throat area at design turbine temperature. The optimum occurs when the throat is opened to 40 percent over design when the turbine temperature is reduced 200° F (111° C) below design. A comparison between the envelope curves of figures 11(b) and (c) shows that they are virtually the same. Thus, there is not likely to be any further gross weight reduction by suppressing both streams instead of only the duct. In fact, the gross weight will very likely increase due to the extra weight of a core suppressor.

A fourth possible configuration would be one with only a core-stream suppressor. This was not examined, however, because it would not be effective at all with duct-burning, where a good suppressor can be used to best advantage. Without duct burning, a core suppressor could not produce a total noise below the duct noise floor, which is indicated in figure 8(b) to be in the vicinity of 104 EPNdB. It could not possibly offer better performance than that of full-stream suppression (fig. 11(c)), which is no better than duct-only suppression (fig. 11(b)).

Plots similar to those of figure 11 were constructed for each of the engines selected for further analysis. For brevity, these plots are not included, but table II summarizes the throat areas found best at two takeoff throttle settings. With the exception of the FPR = 3.5 case with duct stream suppression, these throttle settings are (1) maximum duct burning at 1600° F (871° C) with design turbine temperature and (2) maximum dry (i.e., design T_4 without duct burning). The exception was made for the FPR = 3.5 case with a duct-stream suppressor because an optimization of the type shown in figure 11 showed that the core must be throttled, even when the duct-burner is lit, to derive maximum benefit from a duct suppressor. With all the other turbofan engine designs selected for this study, takeoff operation at design turbine temperature gave results at least as good as those obtained with the core throttled, as long as the duct-burner was lit. The FPR = 3.5 case was exceptional because its bypass ratio of 1.23 was originally selected to provide a high core exit velocity at design T_4 to test the benefit of a core-stream suppressor. When that core-stream suppressor is removed and replaced with a suppressor on the bypass stream, the core must be throttled back so that its noise will not dominate.

At design FPR's of 3.0 and below, suppression of the core stream alone was not considered because the duct stream noise could be made the dominant source at design T_4. At FPR = 3.0, as previously explained, the envelope curves of figure 11 were identical for duct-only and dual-stream suppression, indicating that dual-stream suppression was unnecessary. At FPR = 2.5, a similar comparison of envelope curves revealed likewise that no additional benefit would accrue from suppression of both streams. The additional weight penalty of the unnecessary core suppression would make it undesirable. Because dual-stream suppression was clearly undesirable for engines with low unsuppressed core noise levels, it was not even listed in table II for the FPR = 2.2 case. Only for the FPR = 3.5 case did it appear that dual-stream suppression might be superior to suppression of either stream alone. It is impossible to ascertain if any superiority actually does exist, however, merely by a comparison of the figure 11-type envelope curves because these curves do not appraise the added weight and complexity of dual-stream suppressors.

Although a true optimization was not performed in selecting a design BPR for each FPR (fig. 8(a) to (d)), the manipulation of nozzle throat area at takeoff to more optimally match the engine components for low noise and high thrust compensates to some degree. A significant reduction in computational time and effort was accomplished by this procedure.

The nozzle throat area for the suppressed dry turbojet was opened to the desired takeoff value at various throttle settings. Compressor overspeed was limited to a maximum of 10 percent. Overspeed allowed the engine to swallow more airflow while jet velocity was reduced at any given thrust. Minimization of jet velocity is desirable for noise reduction. The manipulation of throat area permitted thrust improvements at any given noise level in much the same way as with the turbofan engines.

Optimization of Takeoff Wing Loading

Some preliminary results of the complete airplane mission analysis are presented here for the first time in order to show how much of a penalty is incurred by not optimizing wing loading. Subsequent sections of the report concentrate on takeoff gross weight and noise at an estimated optimum wing loading. The baseline airplane on which the aerodynamics were based had a wing loading of 75 pounds per square foot (366 kg/m^2) for the reference 750 000 pound (340 200 kg) gross weight. The results of this study indicate that imposing such a high wing loading requirement could in some cases needlessly penalize the airplane when low noise levels are sought.

Figure 12 shows some of the preliminary mission results for suppressed dry turbojets installed in a 750 000-pound (340 200-kg) airplane. The three curves shown on the plot of range against wing loading represent three different part-throttle power settings. Each throttle setting has an approximately constant sideline noise level associated with it. The noise level is only approximately constant because it changes somewhat with engine size as well as throttle setting, and size changes with wing loading along each curve. The trend to be observed from figure 12 is that the optimum wing loading decreases as throttle setting and, hence, sideline noises are reduced. Furthermore, the penalty for remaining at the reference wing loading of 75 pounds per square foot (366 kg/m^2) grows larger as the takeoff throttle setting (specific thrust) is reduced. The optimum wing loading should not be affected much by scaling the airplane gross weight for a constant 4000-nautical-mile (7408-km) range at each throttle setting. Such scaled airplane data will be presented later.

Data for airplanes scaled for a common 4000-mile range (7408-km) is presented at the FAR 36 noise level for turbojet engines in figure 13. Here, the impact of increasing the required thrust-drag ratio from the reference of 1.2 to 1.4 is shown. The minimum thrust-drag ratio for these airplanes occurs at Mach 2.7 in the climb up to the optimum initial cruise altitude. As the requirement becomes more severe, the optimum wing loading is higher. This is because lower wing loadings (larger wings) force the airplane to a higher initial cruise altitude for best cruise efficiency, but climb thrust margin decreases as altitude is increased. At wing loadings lower than the optimum shown in figure 13, for a 40 percent thrust margin, cruise occurs at an altitude lower than that for peak efficiency, thus penalizing the gross weight. Such considerations are not important with the turbofans since the duct burner can

provide as much thrust augmentation as needed for any reasonable margin.

It would be impractical to present all the wing loading curves for the various turbofan engines in both suppressed and unsuppressed modes. Only a sample, therefore, will be presented for the FPR = 2.5 (BPR = 3.21) case. Curves of range against wing loading are presented for the unsuppressed engine at three throttle settings in figure 14(a). A similar plot is shown in figure 14(b) for this engine with a duct suppressor at four different throttle settings. These curves show that for the turbofan engines, too, the penalty for being at the reference 75 pound-per-square-foot (366-kg/m^2) wing loading instead of the optimum is much more severe at the lower takeoff throttle settings. If the wing loading were not reoptimized for each throttle setting, a false impression would be obtained of the severity of the penalty involved in going to low throttle settings for low noise. The data shown in figure 14 are for airplanes with a takeoff gross weight of 700 000 pounds. The gross weight was reduced from the 750 000-pound (340 200-kg) value of the baseline airplane so that the peaks of these curves would bracket the 4000-mile (7408-km) range desired. The 75-pound-per-square-foot (366-kg/m^2) wing loading no longer has any significance as far as reference aerodynamics are concerned. The baseline aerodynamics are represented by a wing loading of 70 pounds per square foot (342 kg/m^2) (i.e., a planform area of 10 000 ft^2 or 929 m^2) for a 700 000-pound (317 744-kg) airplane. The airframe weight, however, is affected by the weight scaling assumptions and the 70-pound-per-square-foot (342-kg/m^2) wing loading case is not at the reference airframe weight. These airplanes will be scaled later for constant range at the optimum wing loadings.

Effect of Sideline Noise on Takeoff Gross Weight for Design Mission

The effect of sideline noise on takeoff gross weight is shown in figure 15 for suppressed dry turbojet engines. All points shown on the curve represent takeoffs which were throttled to obtain the sideline noise indicated. Noise reductions were obtained by reducing the exhaust jet velocity while simultaneously increasing the engine design airflow to maintain the thrust required for a constant field length. As design airflow is increased, the engine weight increases. Takeoff gross weight must increase as engine weight increases in order to fly a fixed range. Since wing weight, landing gear weight, and engine size and weight are a function of gross weight, they must all be increased to reflect an increase in gross weight. Throttling to reduce noise thus increases the gross weight very rapidly, as shown in figure 15, since engine weight must be increased not just once for noise reasons but again to account for airplane empty weight and fuel load increases. At 108 EPNdB (FAR 36), the gross weight required to fly the nominal 4000-mile (7408-km) range (with the first 600 n mi or 1111 km subsonic) is shown to be 750 000 pounds (340 200 kg). The sea-level-static design airflow required is 690 pounds per second (313 kg/sec) for each of the four turbojet engines. The exhaust gas total temperature for this amount of throttling is 1540° F (838° C), which is below the

postulated suppressor materials limit of 1600° F (871° C). The suppressors are operating at nearly their peak efficiency. The jet exhaust is being suppressed 14.5 PNdB out of a maximum possible of 15 PNdB. The optimum wing loading for each takeoff throttle setting was used in figure 15 (see fig. 12 for these optimums).

The takeoff gross weight against sideline noise plots for some of the turbofan engines of this study are shown in figures 16(a) to (c). The slopes indicated eventually become as steep as that of the turbojet when noise level is reduced. The steep part of the curve is not reached until a lower noise level, however, with the turbofan engines. This minimum acceptable noise level gets lower, too, with progression from the highest to the lowest fan pressure ratio (i.e., as we proceed from fig. 16(a) to (c)). Curves are plotted in figure 16(a) to (c) for the unsuppressed engines as well as suppression cases with only one stream suppressed and with both streams suppressed. With the FPR = 3.5 (BPR = 1.23) engine (fig. 16(a)), single-stream suppression was considered for both the core stream and the duct stream. For the lower FPR cases (figs. 16(b) and (c)), suppression of the core stream alone was not considered for reasons previously discussed. A triangular data point is shown on these curves at the duct temperature limit of 1600° F (871° C) at design T_4 when duct stream suppressors are used. A circular data point indicates the maximum dry (i.e., unaugmented, design T_4) throttle setting. The FPR = 3.5 cases with duct suppression only (fig. 16(a)) were exceptional in that for these cases alone it was better to duct-burn with T_4 throttled back. A hexagonal data point is used to mark the 1600° F (871° C) duct temperature limit in this case where T_4 optimized at 200° F (111° C) below design. A quarter-circle data point is also shown on this curve to mark where the duct-burner is shut off. The optimum T_4 for this condition was 600° F (333° C) below design. Points further to the left on this curve represent still lower levels of takeoff T_4. Points to the left of the circular data points on the other curves represent unaugmented takeoffs at throttled-back conditions below design T_4. Core nozzle throat area was optimized for each throttle setting. Takeoff wing loading was also optimized and was a function of the engine design FPR and BPR, the noise level specified, and the mode of suppression (if any).

Dual-stream suppression produces a gross weight advantage in the FPR = 3.5 engine cases (fig. 16(a)) down to a sideline noise level of about 104 EPNdB. Below this point, suppression of the duct stream alone yields results that are equally as good. Core suppression by itself is seen to provide an improvement over the unsuppressed engines, but the improvement is not nearly as large as that obtained with a duct suppressor. The results shown in figure 16(a) for both dual-stream and core-only suppression cases are slightly optimistic since the core-stream exhaust gas temperature exceeds the postulated 1600° F (871° C) uncooled suppressor materials limit at design T_4. For instance, the core exhaust gas total temperature with the dual-stream suppressors ranges from 1740° F (949° C) to 1815° F (990° C) between the maximum dry and maximum duct-burning

takeoff thrust settings at the optimum core nozzle throat areas. If this temperature is brought down to 1600° F (871° C), only a very slight shift in the dual-stream suppression curve will occur. In fact, below a sideline noise of 107 EPNdB, no shift at all occurs when T_4 is reduced 200° F (111° C) with a simultaneous increase in the amount of duct-burning to keep thrust constant. A gross weight rise of about 6000 pounds (2722 kg) would occur at the right-hand extreme of this curve (i.e., at the triangular data points) when the core exhaust temperature limit is observed. Even with this adjustment, dual-stream suppression still provides lower gross weights than the next-best suppression mode (duct-stream-only suppression) when the added design complexity of a dual-suppressor mechanism are ignored. A somewhat greater upward adjustment in the core-only suppressor curve will occur if it too is limited to a 1600° F (871° C) core exhaust gas temperature. Below a sideline noise of 108 EPNdB, no shift at all occurs. This upward adjustment of the core suppression curve makes duct suppression an even more clear-cut choice than is indicated in figure 16(a) in the single-stream suppression category.

In figure 16(b), dual-stream suppression is shown to be at best a questionable choice when compared to duct-only suppression with the FPR = 3.0 (BPR = 2.00) engine. At dry takeoff settings, dual stream suppression is clearly worse. At the maximum permissible duct temperature, a comparison between the two curves shows that only a very small gross weight reduction (about 1 percent) can be obtained with the added complexity of dual-stream suppressors. Although the unsuppressed engines yield acceptable gross weights at the FAR 36 noise level, a reduction of almost 8 percent can be obtained by duct burning to the 1600° F (871° C) limit with a suppressor. The duct suppressor operates at its peak efficiency, obtaining 15 PNdB of suppression when the duct temperature is at this upper limit. When thrust is reduced to the maximum dry level, only 5.3 PNdB of duct suppression is obtained because of the lower efficiency at the lower exit velocity (as per suppressor schedule of fig. 6).

Figure 16(c) shows the results for engines with FPR = 2.5 and BPR = 3.21. Suppression reduces gross weight by just over 7 percent when the suppressed engines use the maximum allowable amount of duct burning. However, at lower thrust settings (below a duct temperature of about 900° F or 482° C), the unsuppressed engine is better. At these lower duct temperatures the suppressor efficiency is so poor that the noise reduction obtained is insufficient to overcome the disadvantage of the added weight of the suppressor. Since the broken curve for dual-stream suppression lies above the solid duct-only suppression curve at all points, it is unquestionably better to use only duct suppression at FPR = 2.5. The duct suppressor reduces noise 14.2 PNdB at a 1600° F (871° C) duct-stream temperature but only 2.0 PNdB at the maximum dry thrust setting. The suppressor effectiveness tends to decrease as design fan pressure ratio is reduced, since duct exit velocity decreases for any given gas temperature.

Results for the engines having FPR = 2.2 and BPR = 4.18 are not

shown in figure 16 because only two conditions were examined to save computational time. These conditions were maximum duct burning with a duct suppressor and maximum dry takeoff thrust without any suppressor. For the suppressed duct burning condition, a gross weight of 681 000 pounds (308 896 kg) was obtained at a sideline noise of 103.8 EPNdB. For the maximum dry unsuppressed case, a gross weight of 813 000 pounds (368 770 kg) was obtained at a noise level of 96.8 EPNdB.

The preceding results for suppressed duct burning at the limit of 1600° F (871° C) and the best nonduct-burning cases, both suppressed and unsuppressed, are summarized in figure 17(a). The dry turbojet curve from figure 15 is also included for comparison. The turbofan curves shown here are envelopes of the best data (i.e., lowest gross weight at any noise level) from figure 16. It is clear from figure 17(a) that duct burning to the 1600° F (871° C) maximum limit during takeoff is advantageous from a gross weight standpoint. For the range of engine design variables examined, the gross weight is reduced about 7 percent at any given noise level by duct burning to the upper limit with suppression. The curve for suppressed duct-burning takeoff cases turns up rapidly as the sideline noise is reduced below 105 EPNdB. This point corresponds to an engine with FPR = 2.5, as can be seen from figure 17(b). It would not be wise to design for a duct-burning takeoff much below 105 EPNdB because of the high gross-weight penalty exacted for further noise reductions. It also appears from the trends of the curves in figure 17(a) that the duct-burning and the no-duct-burning curves are starting to converge below 104 EPNdB. Since the lowest duct-burning data-point is at 103.8 EPNdB (for an FPR = 2.2 engine), the duct-burning takeoff curve of figure 17(a) has not been extended any further to the left.

Figure 17(a) suggests too that at very low noise levels it would be well to design the duct-burning turbofan engines not to rely on duct burning at takeoff. Furthermore, the use of suppressors without allowing duct burning (broken curve, fig. 17(a)) is detrimental at noise levels below 106 EPNdB. Suppressor efficiency is so low that the amount of suppression obtained is not worth the weight penalty and thrust loss incurred by their use. Even above 106 EPNdB there is no advantage to using suppression without duct-burning. The point of greatest noise on the broken curve was produced by the FPR = 3.5 engine with core suppression only at a sideline noise of 108.8 EPNdB. The gross weight obtained with these engines is only about 0.1 percent less than that obtained with unsuppressed engines of FPR = 3.05 (the FPR obtained from fig. 17(b) at the same noise level). But the element of risk and the complexity is much greater with engines designed to use a suppressor. In a case such as this where there is no significant advantage for taking such a risk and increasing the complexity, a designer should choose the unsuppressed engine with the lower FPR and higher BPR. At these higher noise levels, however, duct-burning to the 1600° F (871° C) limit appears to be beneficial when the noise is controlled with suppressors. The payoff in reduced gross weight seems to outweigh the additional risk and complexity of the suppressor. The answer to the pollution question with duct-burning in takeoff is still uncertain and could possibly force consideration of only

nonaugmented takeoffs. Such a consideration would make the suppressed dry turbojet more of a contender. From figure 17(a), it appears to be competitive with the turbofan without duct-burning in takeoff if noise levels are allowed to approach 111 EPNdB. But at FAR 36 and below it seems to be a poor choice due to the steepness of the gross-weight-against-noise curve.

Figure 17(b), which has already been referred to, shows the design fan pressure ratio schedule against noise for turbofan engines having unsuppressed takeoffs with no duct-burning and suppressed takeoffs with maximum duct burning. The circled points along the two curves represent the engines considered in the matrix. The bypass ratios of these selected engines have been previously correlated to fan pressure ratio in figure 9.

The sea-level-static engine design airflows of the turbofan and turbojet engines used in figure 17(a) have been plotted against sideline noise in figure 17(c). The engine size is inversely related to specific thrust at takeoff. The suppressed engines of both types (i.e., turbofan as well as turbojet) tend to have higher specific thrusts than unsuppressed turbofans at the same noise level. A smaller engine size thus results for the suppressed engines. The suppressed dry turbojet airplanes, though, have significantly higher gross weights than the suppressed turbofans which duct-burn at takeoff. The turbojet engine size would have been much greater relative to the suppressed duct-burning engines if there had not been a difference in the optimized takeoff wing loading. At the FAR 36 sideline noise level of 108 EPNdB, the wing loading for the suppressed fans with duct burning was 65 pounds per square foot (318 kg/m^2) while that for the turbojet-powered airplanes was only 58 pounds per square foot (283 kg/m^2). The lower wing loading (larger wing) used for the turbojets allows their size to be smaller. Differences in the wing and engine size trades between these two suppressed engine types arose primarily because of the difference in engine weight density.

The impact that the wing loading optimization has on the gross weight results related to sideline noise is shown in figure 18 for two extremes. In addition to the two extreme curves having optimized wing loadings (replotted from fig. 17(a)), figure 18 also shows for comparison corresponding curves with wing loading fixed at the reference value of 75 pounds per square foot (366 kg/m^2). The wing loading optimization has the most effect on the results obtained for the dry turbojet and the least on the suppressed turbofans having maximum allowable augmentation during takeoff. The turbojet pair of curves has a greater difference between them than the turbofan curves have because the turbojet weight per unit of allowable takeoff thrust is higher at each sideline noise level. Since the engine weight per unit of allowable thrust is higher for the turbojet, a greater potential improvement exists for reducing the takeoff thrust required by reducing the wing loading. The spread between the two turbofan curves does not increase as rapidly as it does for the turbojet when noise is decreased because design bypass ratio is continuously in-

creased to minimize the engine weight as specific thrust decreases. The turbojet experiences no such relief as takeoff noise and specific thrust are reduced - the engine weight is approximately inversely proportional to allowable takeoff specific thrust.

One reason for showing some results with a constant wing loading is that many simplifying assumptions were made concerning aerodynamic changes resulting from configurational changes. Additional assumptions were made concerning the effect of these configurational changes and changes in design gross weight on empty weight. While the 75-pound-per-square-foot (366-kg/m^2) wing loading no longer truly represents the aerodynamic reference once the gross weight is changed from 750 000 pounds (340 200 kg), and component weight assumptions also become involved once gross weight is changed, less divergence from a reference point occurs with a fixed wing loading. Hence, the constant wing loading results shown in figure 18 are less subject to question than those with the optimized wing loading. Although the gross weights are higher with the constant wing loading, the conclusions concerning the best engine cycles are not changed. If anything, they are reinforced because the gross weight increment from the best to the worst increases. Although the constant wing loading curves are less subject to question, a comparison with the optimized wing loading curves leads to the conclusion that perhaps a false impression of the severity of the penalty for low noise may be obtained if no attempt is made to optimize wing loading. A more rigorous analysis of the effect of wing loading is recommended to substantiate the benefits found for its optimization in this study.

Effect of Sideline Noise on Direct Operating Cost for Design Mission

Direct operating cost has been computed for the minimum gross weight envelope curves of figure 17(a) by the standard Air Transport Association formula (ref. 17). The results of these calculations are shown in figure 19 for two different fuel costs. The lower fuel cost of 16 cents per gallon ($42.20/$m^3$) is shown because, prior to the Arab oil embargo beginning in the fall of 1973, it was representative of the upper limit of fuel prices then prevailing for airline customers (ref. 18). Another fuel price of 35 cents per gallon ($92.50/$m^3$) is also shown to indicate how the engine comparison is affected by higher fuel prices, since post-embargo prices may eventually stabilize in the time period of interest at some price in this vicinity.

The curves of figure 19 show that the superiority of the suppressed duct burning turbofans relative to the other engines escalates as the fuel price increases. At the FAR 36 sideline noise level of 108 EPNdB, the lower set of curves indicates that the suppressed dry turbojets are slightly superior to the unsuppressed turbofans with fuel at 16 cents per gallon ($42.20/$m^3$). The upper set of curves shows that at this noise level the unsuppressed turbofans are better than the suppressed turbojets. As sideline noise is reduced, the turbojets are relatively more inferior due to the more rapid increase in gross weight for turbojet-powered air-

planes.

In terms of DOC, the turbojet results seem somewhat more competitive than might be expected from the gross weight plot of figure 17(a). This is because the specific propulsion pod cost was taken as \$167 per pound (\$368/kg) for the turbojets instead of the higher \$232 per pound (\$511/kg) value assumed for all of the turbofans. These figures are based on admittedly crude empirical data but are an attempt to reflect the greater design simplicity of the basic turbojet. The specific airframe cost was taken as \$178 per pound (\$392/kg) regardless of engine type or wing loading.

The resultant DOC's plotted in figure 19 may seem to be bunched rather close together at a given fuel price. But if the differences shown were real, they could be quite significant to an airline. A DOC difference of only 0.1 cent per seat-mile (0.062 cent/seat-km) corresponds to \$500 million per year for a fleet of 500 supersonic transports.

Effect of Subsonic Cruise Requirement on Mission Results

One of the mission ground rules for these studies was that the design 4000-mile (7408-km) mission was to include an initial subsonic range of 600 miles (1111 km). The purpose of this section of the report is to determine the effect of the subsonic requirement on the mission results for both the turbojet and one of the better duct-burning turbofan engines. The duct-burning turbofan engine used in this perturbation to the basic study is the FPR = 3.0 (BPR = 2.00) version with a suppressed duct. Takeoff duct temperature was set to the limit of 1600° F (871° C). An equal sideline noise constraint of approximately FAR 36 + 1 EPNdB was used for both engine types. Airplane wing loading was not optimized but was set at the 75-pound-per-square-foot (366 kg/m^2) reference value.

The two solid curves of figure 20(a) show how the design gross weight varies with initial subsonic design range for both engine types when the total range is fixed at 4000 nautical miles (7408 km). The right hand extremities of these two curves represent the nominal design mission with a 600-mile (1111-km) initial subsonic range. The left-hand extremities represent design missions flown with no initial subsonic cruise. The initial subsonic range shown for the latter two points represents the range used in climb and acceleration up to Mach 1.0. It takes more range for the turbofan to climb and accelerate to Mach 1.0 than it does for the turbojet due to the turbofan's higher thrust lapse rate over this speed range. For both engine types, figure 20(a) shows that the design gross weight decreases as the initial subsonic requirement is reduced. As the difference in the slope between the two curves indicates, the turbojet's gross weight is more adversely affected by an initial subsonic cruise requirement than the turbofan's. This is because the turbojet subsonic cruise sfc is not as low as that of the turbofan (see throttle curve of fig. 10(b)). Because the turbofan cruises at the maximum thrust setting permitted without turbine cooling bleed, it can take full advantage of

its better potential subsonic cruise sfc.

The two broken curves of figure 20(a) represent the gross weights needed for the two different engine types for a constant off-design total range of 2500 miles (4630 km) with an initial subsonic range of 400 miles (741 km). The subsonic range of the off-design mission is constant at 400 miles (741 km) regardless of the subsonic design range indicated by the abscissa. This particular off-design mission was chosen because the market analysis of reference 19 indicates that if the design range is 4000 nautical miles (7408 km), the average range per flight for a fleet of airplanes will be 2500 miles (4630 km), of which about 400 miles (741 km) will be subsonic. In figure 20(a), the airplane structure and engines are fixed at the values set for the design mission when the off-design mission is flown. The off-design gross weights (broken curves) are lower only because fuel was off-loaded for the shorter off-design range. The design subsonic range requirement has a reduced impact on the results for the off-design mission, compared to the design mission. The design subsonic range specification has almost no influence on the off-design-mission gross weight for the turbofan. For the turbojet, however, the effect is still of some significance.

The results of figure 20(a) are shown in terms of direct operating cost in figure 20(b). A fuel cost of 35 cents per gallon ($92.50/m^3$) was used in these calculations. In this plot, the off-design DOC is worse than the design despite the lower fuel requirement and reduced gross weight. The fuel consumed per mile is not significantly reduced, however, for the off-design mission. At the right-hand end of the turbojet curves (fig. 20(b)), approximately the same amount of fuel was burned per mile on both the design and off-design missions. More fuel was burned per mile for the off-design mission relative to the design at the left-hand end of these curves. The turbofan off-design mission saves some fuel over design on a per mile basis at the right-hand end of the figure but not at the left-hand end. There are certain costs that accrue with time regardless of range or fuel consumption. Since DOC is computed on a per-unit-range basis, these cost components rise if block speed goes down. The block speed was lower for the off-design mission than it was for the design in all cases considered, although the disparity between the two narrows as we proceed to the right on the curves. The direct operating cost components which were adversely affected by the reduced block speed of the off-design mission included depreciation, flight crew, insurance, and direct maintenance charges.

The curves of figure 20(b) show that the turbojet is adversely affected by a DOC comparison based on the off-design average mission instead of the design mission. The turbojet is still sensitive to the value of the initial subsonic design range, even on the off-design mission which has a constant subsonic requirement. The turbofan is relatively insensitive to design subsonic range on the off-design mission. Although the DOC is closer between the turbofan and turbojet with no design subsonic cruise, the turbofan is still clearly superior, even at this condition.

CONCLUDING REMARKS

A comparative study was made of parametric duct-burning turbofan and suppressed dry turbojet engines installed in a 234-passenger supersonic transport. The turbofan engines were analyzed for a range of fan pressure ratios from 2.2 to 3.5. These separated-flow dual-stream engines were considered both with and without jet noise suppressors. The design parameters that would produce the best mission results were selected for sideline noise levels of FAR 36 (108 EPNdB) and below. The total range was fixed at 4000 nautical miles (7408 km) and takeoff gross weight, the primary figure of merit, was allowed to vary with choice of engine, takeoff throttle setting, and takeoff wing loading. Tradeoffs between takeoff thrust loading and wing loading were evaluated over the sideline noise spectrum for a constant 10 500-foot (3200-m) FAR takeoff field length. The relatively high altitude obtained at the 3.5-mile (6.5-km) community fly-over noise measurement station with this field length tends to make the sideline noise the dominant noise criterion when the thrust at the community point is reduced for the minimum climb gradient permitted by FAR 36.

In this study, trades between lower takeoff thrust and larger wings were emphasized because of the large engine sizes that would otherwise be required to obtain a constant takeoff field length at low values of sideline noise. The large engine sizes lead to large engine weights and large installation drags. Simplifying assumptions were made with regard to the effect of wing area changes on aerodynamics and operating empty weight in the airplane evaluation. The turbojet engines benefited the most from the wing area-engine size trades because they had the highest engine weight per unit of airflow at any given noise level. The suppressed duct-burning turbofan engines using duct burning during takeoff benefited the least from these trades. The optimum wing loading declined as sideline noise was reduced. The optimum was also influenced by the type of engine and the level of suppression. Increasing the level of suppression available with a given engine tends to increase the optimum wing loading for a given level of sideline noise. Although these wing area-engine size trades were important in determining the minimum level of takeoff gross weight for each engine type over the noise spectrum, the changes were not sufficient to change the ranking of the engines at any noise level.

The suppressed duct-burning turbofan engines with duct burners on at takeoff produced the lowest gross weights from FAR 36 down to about FAR 36 - 4 EPNdB. At FAR 36, they produced gross weights as much as 13 percent below the 750 000 pounds (340 200 kg) achieved with the suppressed dry turbojets. Below FAR 36, the comparison becomes even more unfavorable to the dry turbojet. If sideline noise levels below about FAR 36 - 4 EPNdB are desired, unsuppressed duct-burning turbofan cycles without duct burning during takeoff are best. The use of a suppressor was found to be of no benefit to the duct-burning turbofan when unaugmented takeoffs were used. This was found to be true at a given noise level even when the cycle was reoptimized to achieve maximum benefit from

a suppressor.

In general, for a given mode of suppression, design fan pressure ratio tends to decline and design bypass ratio tends to increase as sideline noise is reduced. At a given noise level, the fan pressure ratio of the optimized suppressed turbofan cycle is higher than it is for an unsuppressed cycle. The corresponding bypass ratio is lower for the suppressed cycle because of the inverse relation between FPR and BPR.

Below about FAR 36 - 3 EPNdB sideline noise, the gross weight penalty becomes rather severe for further noise reduction. For example, at FAR 36 - 6 EPNdB the gross weight of the optimum duct-burning turbofan (at this noise level, it is unsuppressed and unaugmented in takeoff) produces a takeoff gross weight of 750 000 pounds (340 200 kg) - equal to that achieved by the suppressed dry turbojet at FAR 36, but approximately 13 percent higher than that achieved by the optimum duct-burning turbofan cycle at FAR 36 - 3 EPNdB (at this noise level, the optimum cycle is suppressed and augmented at takeoff). Hence, at least for this type of engine, the gross weight penalty is quite severe when a noise level below a certain minimum is specified - in spite of fact that the cycle was reoptimized for each noise level. The industry and regulatory authorities should be aware of where these minimum noise levels are so that gross weight and, hence, economic penalties will not be unduly incurred for small noise benefits.

The optimum suppressor mode for the duct-burning turbofan cycles with augmented takeoffs was either a combination of duct and core stream suppression or duct-only suppression. At the highest fan pressure ratio considered (i.e., FPR = 3.5), there was a slight advantage for dual-stream suppressors. For all the other turbofan cycles, the optimum results occurred with duct-only suppression. Core-only suppression was beneficial in a limited sense only with the 3.5 FPR case when the duct-burner was turned off at takeoff. It was beneficial with this no-augmentation restriction only in comparison with the other modes of suppression. Equal results were obtained by a cycle reoptimized for no suppressor.

The widely used SAE jet noise calculation procedures were used in this study. Different answers would be obtained if other methods were used. As recommended by the procedure, the full forward velocity of the airplane was subtracted from the jet velocity in obtaining a shear velocity with which to compute sound pressure level. This relative velocity noise credit is perhaps only partially obtained in actuality. In this respect, the procedure used herein may produce somewhat optimistic results. Other aspects of the calculation procedure were somewhat conservative. No engine masking, extra ground attenuation, or time duration benefit was assumed in the sideline EPNdB calculations. In the coannular-exhaust turbofan engines, each stream was assumed to generate noise independently of the other, with the combined noise being the result of adding antilogarithmically the noise of the two streams. These noise

calculation techniques are simplified and approximate, but further refinement is probably unjustified due to the tentative nature of much of the available empirical noise data and the broad spectrum of engine design parameters that were considered. Little empirical noise data is available, for example, for coannular exhausts with the outer stream velocity higher than the inner stream, as was the case with the suppressed turbofans found most attractive in this study. Much unjustified extrapolation from the noise data is required to simulate such a situation in more elaborate calculation procedures designed to include an interactive effect between the inner and outer streams.

APPENDIX - SYMBOLS

A	cross sectional area, ft^2 (m^2)
BPR	bypass ratio
C_D	drag coefficient
C_f	friction coefficient
C_L	lift coefficient
C_{L_O}	lift coefficient where $C_{D_{min}}$ occurs
D	drag, lb (N)
DBTF	duct-burning turbofan
F_n	net thrust, lb (N)
FAR	Federal Air Regulation
FPR	fan pressure ratio
M	free-stream Mach number
Re	Reynolds number at free-stream conditions
S	projected wing or tail planform area or body or nacelle surface area, ft^2 (m^2)
sfc	specific fuel consumption, lb/hr/lb (kg/sec/N)
T	temperature, ^oF (^oC)
TJ	turbojet
W	weight, lb (kg)
$\dot{W}$	engine airflow, lb/sec (kg/sec)

Subscripts:

af	airframe
c	corrected
des	design
eng	engine

f	friction
g	gross, takeoff
ht	horizontal tail
i	induced, due to lift
ic	incompressible flow
ℓg	landing gear
min	minimum
nac	nacelle
p	pressure or wave
prop	propulsion system
vt	vertical tail
w	wing
2	fan face station in turbofan engines and compressor face in turbojet engines
4	turbine rotor-inlet station
8	primary exhaust nozzle throat station
24	duct-burner station in duct-burning turbofan engines

REFERENCES

1. Whitlow, John B., Jr.: Comparative Performance of Several SST Configurations Powered by Noise Limited Turbojet Engines. NASA TM X-68178, 1972.

2. Whitlow, John B., Jr.; Weber, Richard J.; and Civinskas, Kestutis C.: Preliminary Appraisal of Hydrogen and Methane Fuel in a Mach 2.7 Supersonic Transport. NASA TM X-68222, 1973.

3. Szeliga, R.; and Allan, R. D.: Advanced Supersonic Technology Propulsion System Study. (R74AEG330, General Electric Co.; NAS 3-16950), NASA CR-143634, 1974.

4. Sabatella, J. A., ed.: Advanced Supersonic Propulsion Study - With Emphasis on Noise Level Reduction. (PWA TM-4871, Pratt & Whitney Aircraft; NAS 3-16948), NASA CR-134633, 1974.

5. Struck, H. G.; and Butsko, J. E.: Booster Wing Geometry Trade Studies. NASA Space Shuttle Technology Conference. Volume I - Aerothermodynamics, Configurations, and Flight Mechanics, NASA TM X-2272, 1971, pp. 611-642.

6. Matting, Frid W.; Chapman, Dean R.; Nyholm, Jack R.; and Thomas, Andrew G.: Turbulent Skin Friction at High Mach Numbers and Reynolds Numbers in Air and Helium. NASA TR R-82, 1961.

7. Koenig, Robert W.; and Kraft, Gerald A.: Influence of High-Trubine-Inlet-Temperature Engines in a Methane-Fueled SST When Takeoff Jet Noise Limits Are Considered. NASA TN D-4965, 1968.

8. Koenig, Robert W.; and Fishbach, Laurence H.: GENENG - A Program for Calculating Design and Off-Design Performance for Turbojet and Turbofan Engines. NASA TN D-6552, 1972.

9. Livinghood, John N. B.; Ellerbrock, Herman H.; and Kaufman, Albert: 1971 NASA Turbine Cooling Research Status Report. NASA TM X-2384, 1971.

10. Denning, R. M.; and Hooper, J. A.: Prospects for Improvement in Efficiency of Flight Propulsion Systems. J. Aircraft, vol. 9, no. 1, Jan. 1972, pp. 9-15.

11. Gerend, Robert P.; and Roundhill, John P.: Correlation of Gas Turbine Engine Weights and Dimensions. AIAA Paper 70-699, June 1970.

12. Corning, Gerald: Supersonic and Subsonic Airplane Design. 2nd ed., Edwards Bros., Inc., 1960.

13. Jet Noise Prediction. Aerospace Information Rept. 876, SAE, July 10, 1965.

14. Definitions and Procedures for Computing the Perceived Noise Level of Aircraft Noise. Aerospace Recommended Practice 865, SAE, Oct. 15, 1964.

15. Dunn, D. G.; and Peart, N. A.: Aircraft Noise Source and Contour Estimation. (D6-60233, Boeing Commercial Airplane Co.; NAS 2-6969), NASA CR-114649, 1973.

16. Boeing's Latest SST Proposal. Part I. Flight International, vol. 95, no. 3123, Jan. 16, 1969, pp. 104-108.

17. Standard Method of Estimating Comparative Direct Operating Costs of Turbine Powered Transport Airplanes. Air Transport Assoc. of America, Dec. 1967.

18. Jet Fuel Prices Rising in Europe. Aviation Week & Space Tech., vol. 98, no. 4, Jan. 22, 1973, p. 19.

19. "Studies of the Impact of Advanced Technologies Applied to Supersonic Transport Aircraft. Volume III - Market Analysis (Task II)," D6-22529-2, Apr. 1973, Boeing Commercial Airplane Co., Renton, Washington.

TABLE I. - SEA-LEVEL-STATIC DESIGN POINT CHARACTERISTICS

COMMON TO ALL STUDY ENGINES

Characteristic	Turbojet	Turbofan
Inlet pressure recovery	0.960	0.960
Overall fan-compressor pressure ratio	10.0	10.0
Fan adiabatic efficiency, percent	----	85
Inner compressor adiabatic efficiency, percent	85	87
Power extraction per 1000 lb/sec (454 kg/sec) airflow, hp (kW)	133 (99.2)	133 (99.2)
Turbine rotor inlet temperature, ^{o}F (^{o}C)	2725 (1496)	2725 (1496)
Pressure ratio across primary burner	0.944	0.944
Primary burner efficiency, percent	98.5	98.5
Duct burner efficiency, percent	----	93
Pressure ratio across duct burner	----	0.94
Cycle chargeable turbine cooling bleed, percent of core flow	8.7	9.2-10.5
H-P turbine adiabatic efficiency, percent	90	90
L-P turbine adiabatic efficiency, percent	----	90
Tailpipe pressure loss (core stream), $\Delta P/P$	0.02	0.02
Nozzle gross thrust coefficient (unsuppressed)	0.98	0.98

TABLE II. - OPTIMUM CORE NOZZLE THROAT AREA DURING TAKEOFF FOR TURBOFAN ENGINES

FPR	BPR	Type suppressor	$A_8/A_{8_{des}}$	
			$T_{d/b}$ = 1600° F (871° C)	Maximum dry
3.5	1.23	None	----	1.30
		Core stream	1.05	1.00
		Duct stream	[a]1.50	[b]1.50
		Dual stream	1.10	1.30
3.0	2.00	None	1.10	1.30
		Duct stream	1.50	1.50
		Dual stream	1.00	1.20
2.5	3.21	None	1.00	1.30
		Duct stream	1.30	1.40
		Dual stream	1.00	1.30
2.2	4.18	None	----	1.20
		Duct stream	1.20	----

[a] T_4 reduced 200° F (111° C) from design.

[b] T_4 reduced 600° F (333° C) from design.

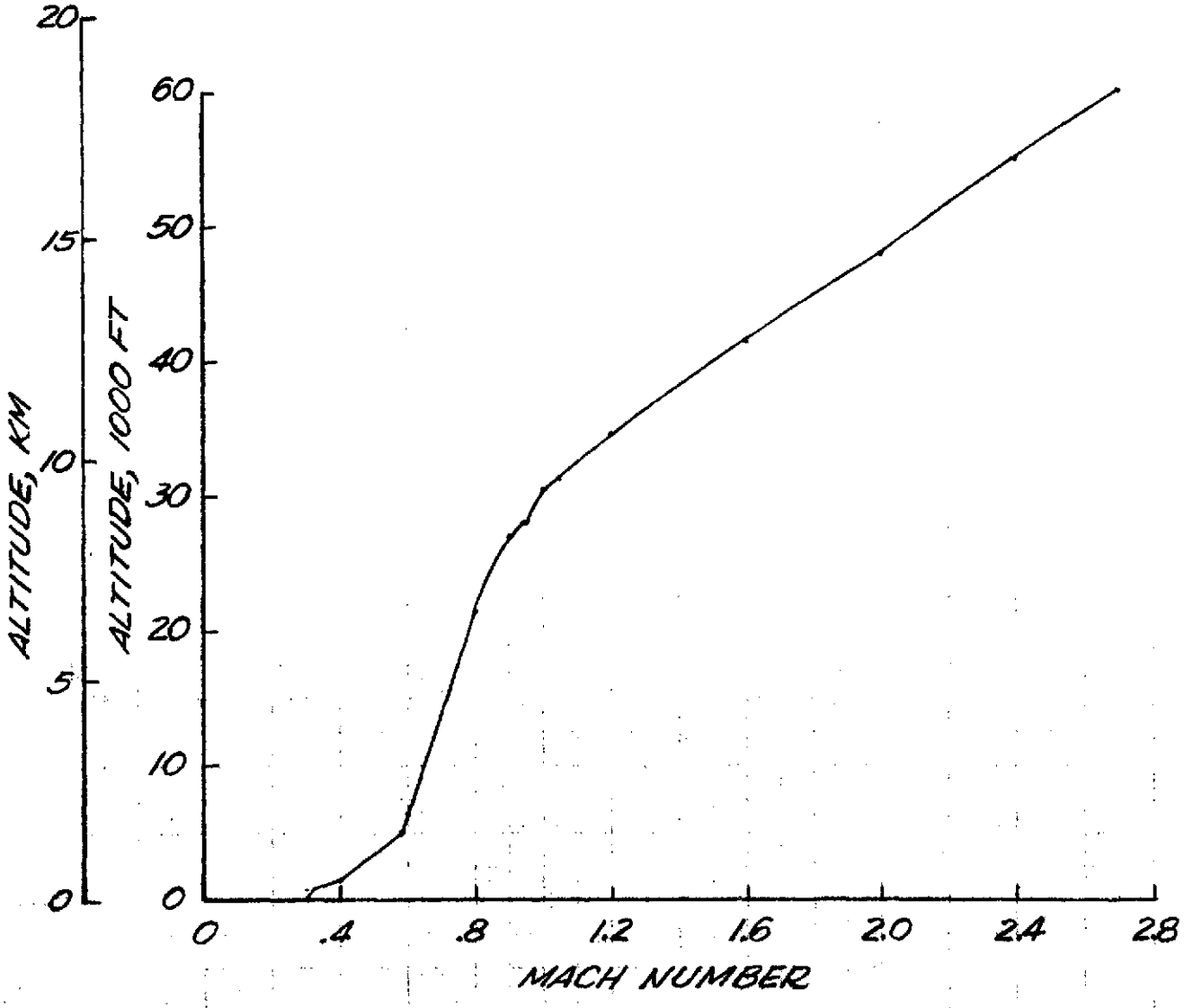

FIGURE 1. - CLIMB/ACCELERATION MACH NUMBER - ALTITUDE SCHEDULE.

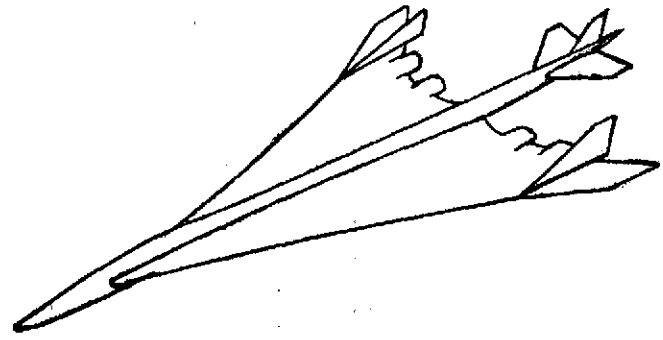

FIGURE 2. – SKETCH OF NASA-LANGLEY BASELINE CONFIGURATION FOR MACH 2.7 CRUISE AIRPLANE.

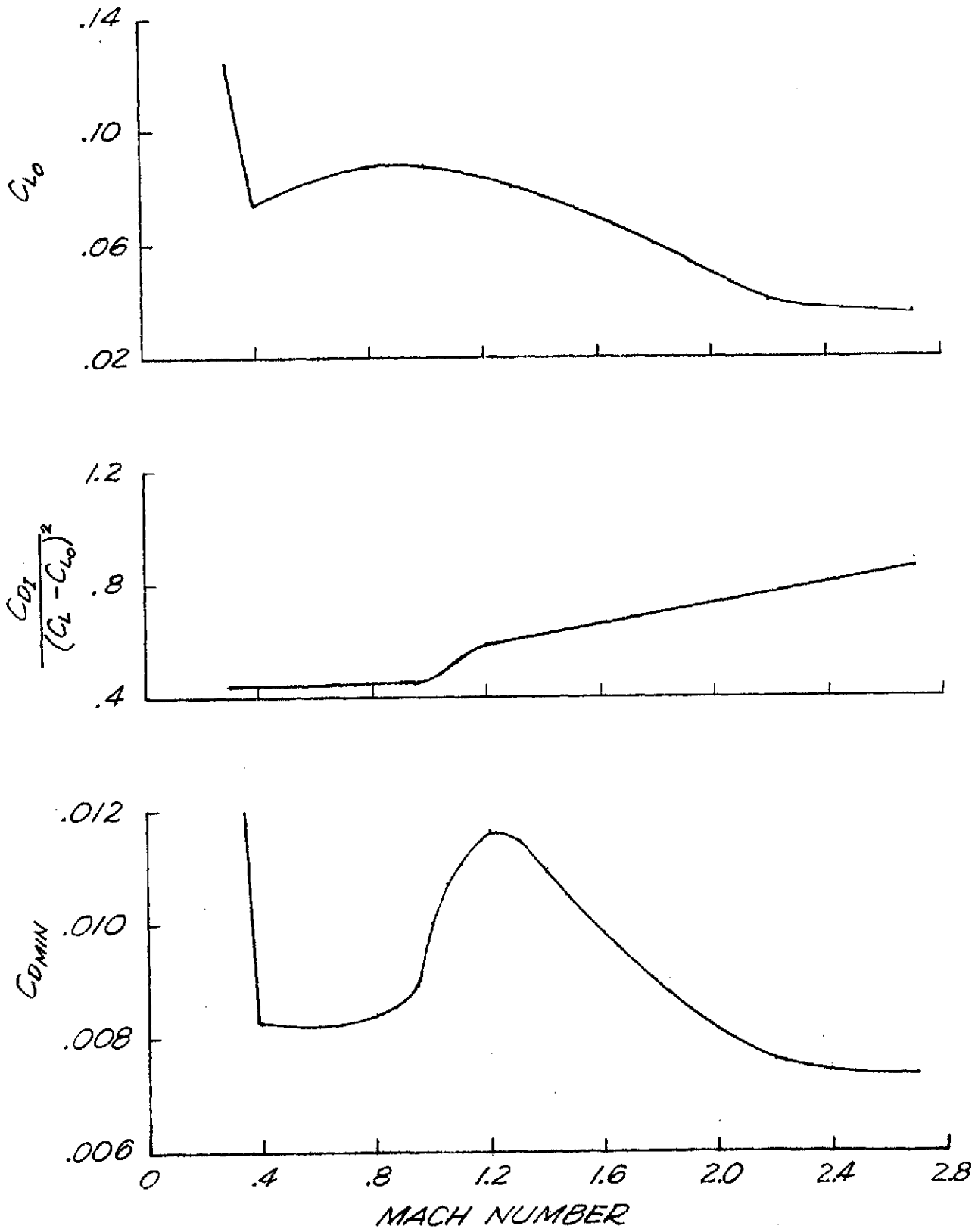

FIGURE 3. —REFERENCE AERODYNAMICS FOR 234-SEAT ARROW-WING AIRPLANE BASED ON 10 000 FT^2 (929 M^2) WING AREA. INCLUDES 633 LB/SEC (287 KG/SEC) TURBOJET NACELLES.

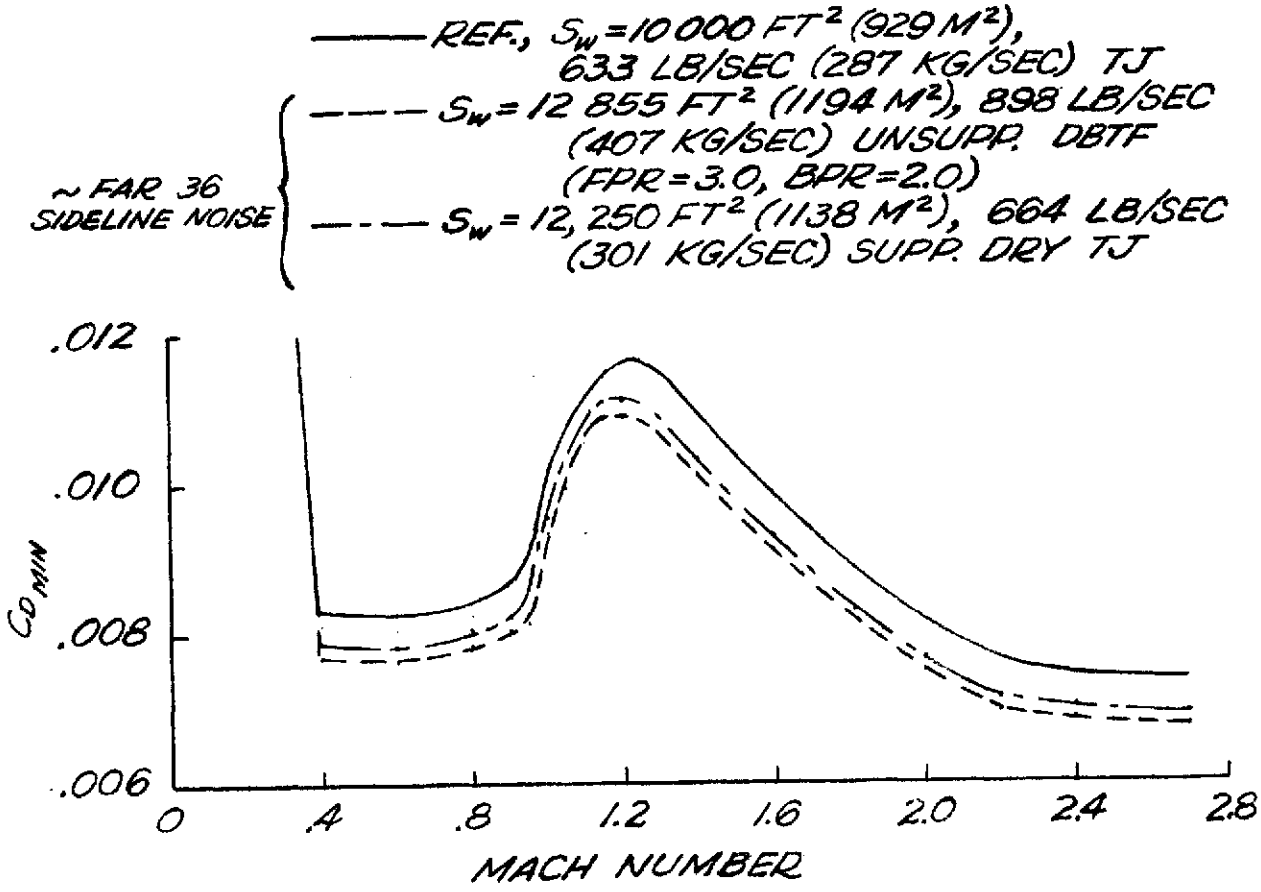

FIGURE 4. – COMPARISON OF TYPICAL SCALED $C_{D_{MIN}}$ SCHEDULES WITH REFERENCE FOR 234-SEAT ARROW-WING AIRPLANE.

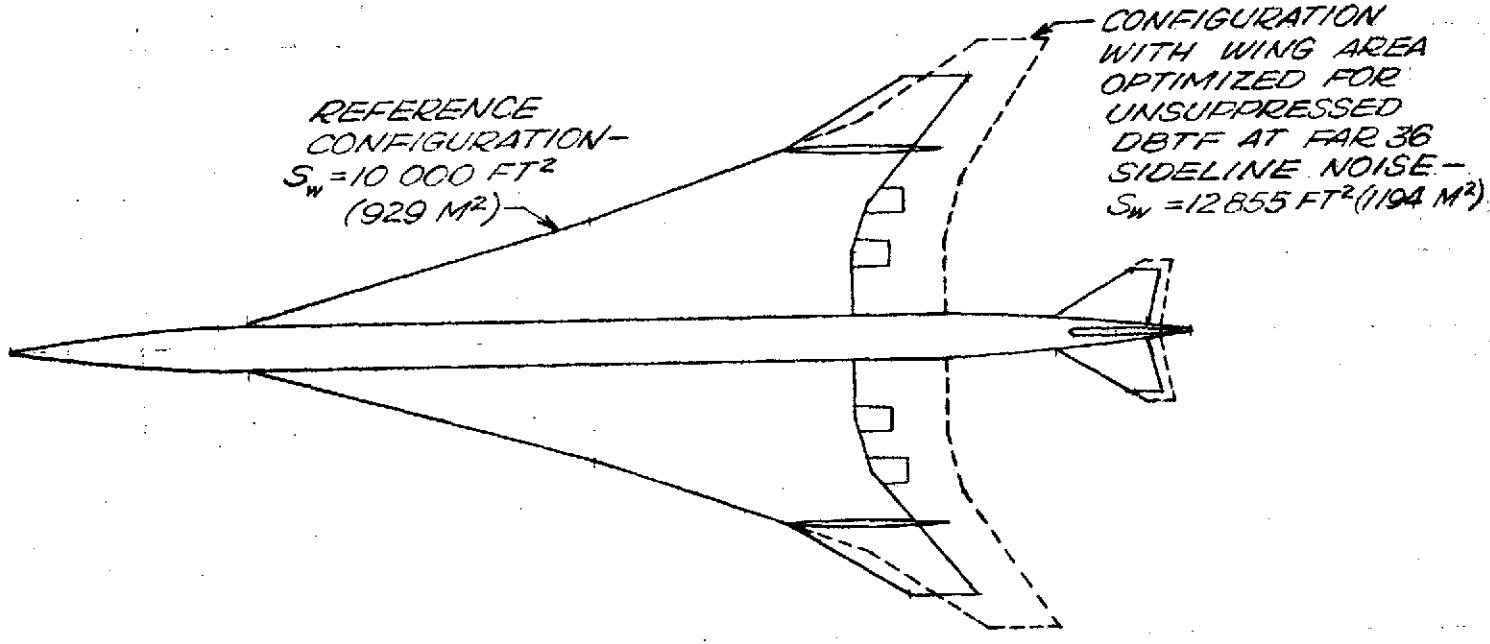

FIGURE 5.-ILLUSTRATION OF CONFIGURATIONAL CHANGES THAT ARISE FROM TAKEOFF THRUST AND WING LOADING TRADE-OFFS. 234-SEAT ARROW-WING AIRPLANE. FIXED WING ASPECT RATIO AND FUSELAGE DIMENSIONS.

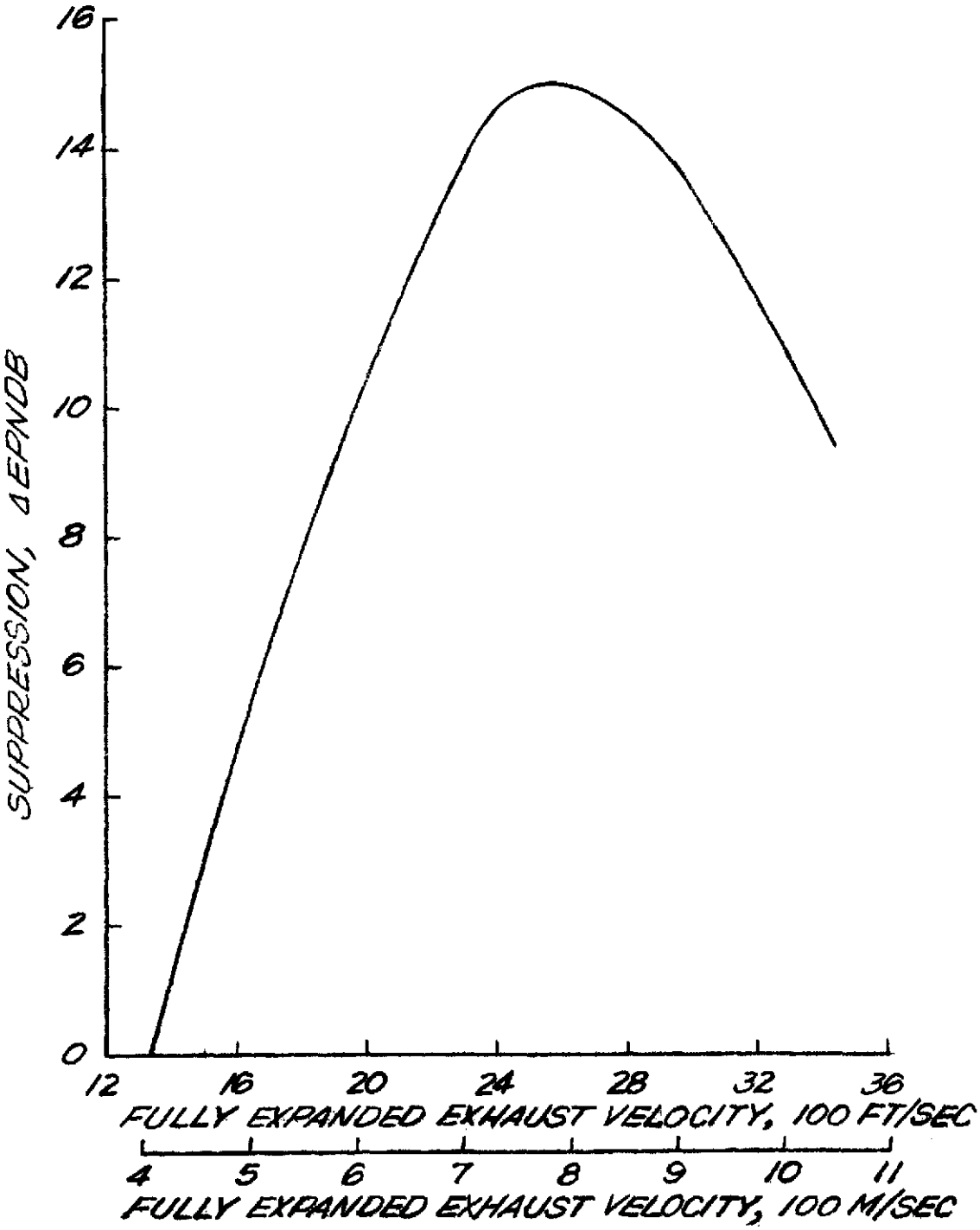

FIGURE 6. – SUPPRESSOR CHARACTERISTIC CURVE.

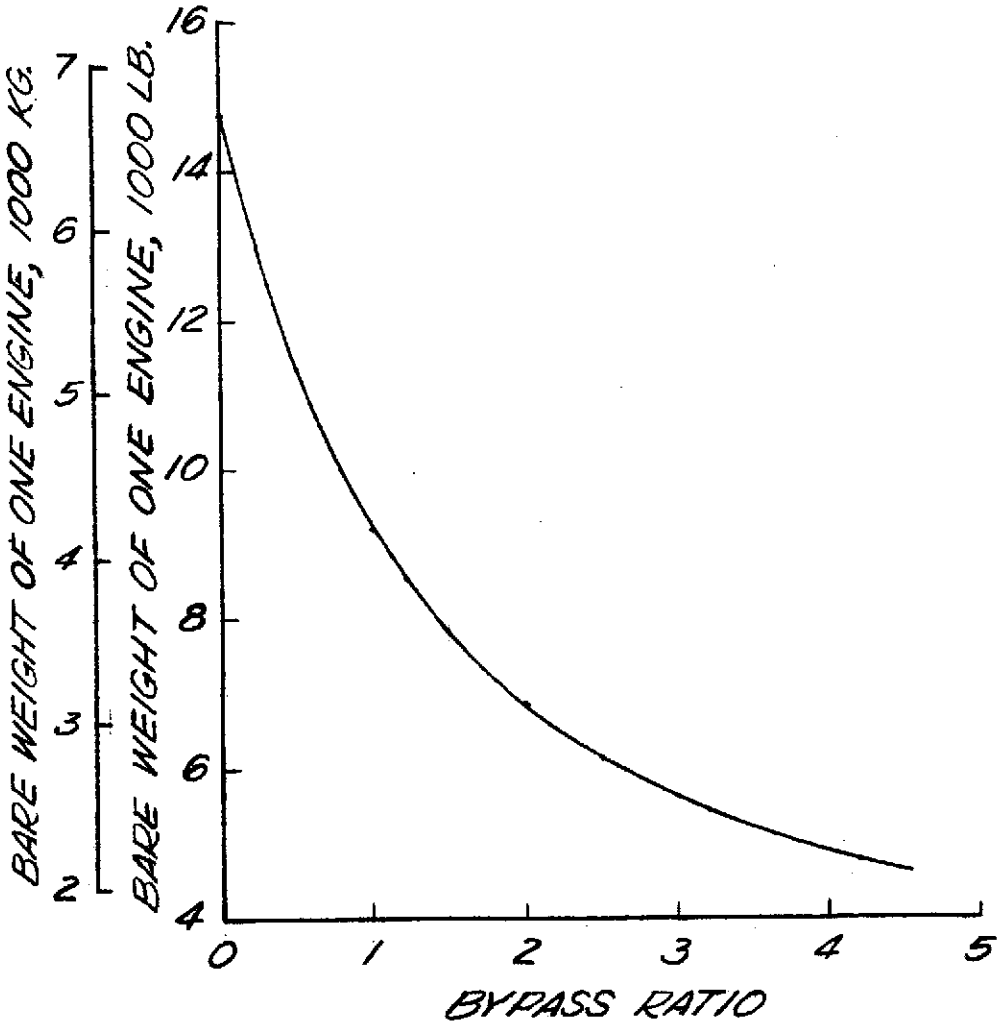

FIGURE 7. – BARE ENGINE WEIGHT RELATED TO BPR FOR 1000 LB/SEC (454 KG/SEC) SIZE, AS PREDICTED BY GEREND AND ROUNDHILL (REF. 11) FOR ADVANCED TECHNOLOGY ENGINES OF THIS STUDY. DOES NOT INCLUDE DUCT BURNERS, EXHAUST NOZZLE/SUPPRESSOR, ACCESSORIES, ETC. OPR = 10, TURBINE TEMPERATURE = 2725°F (1496°C).

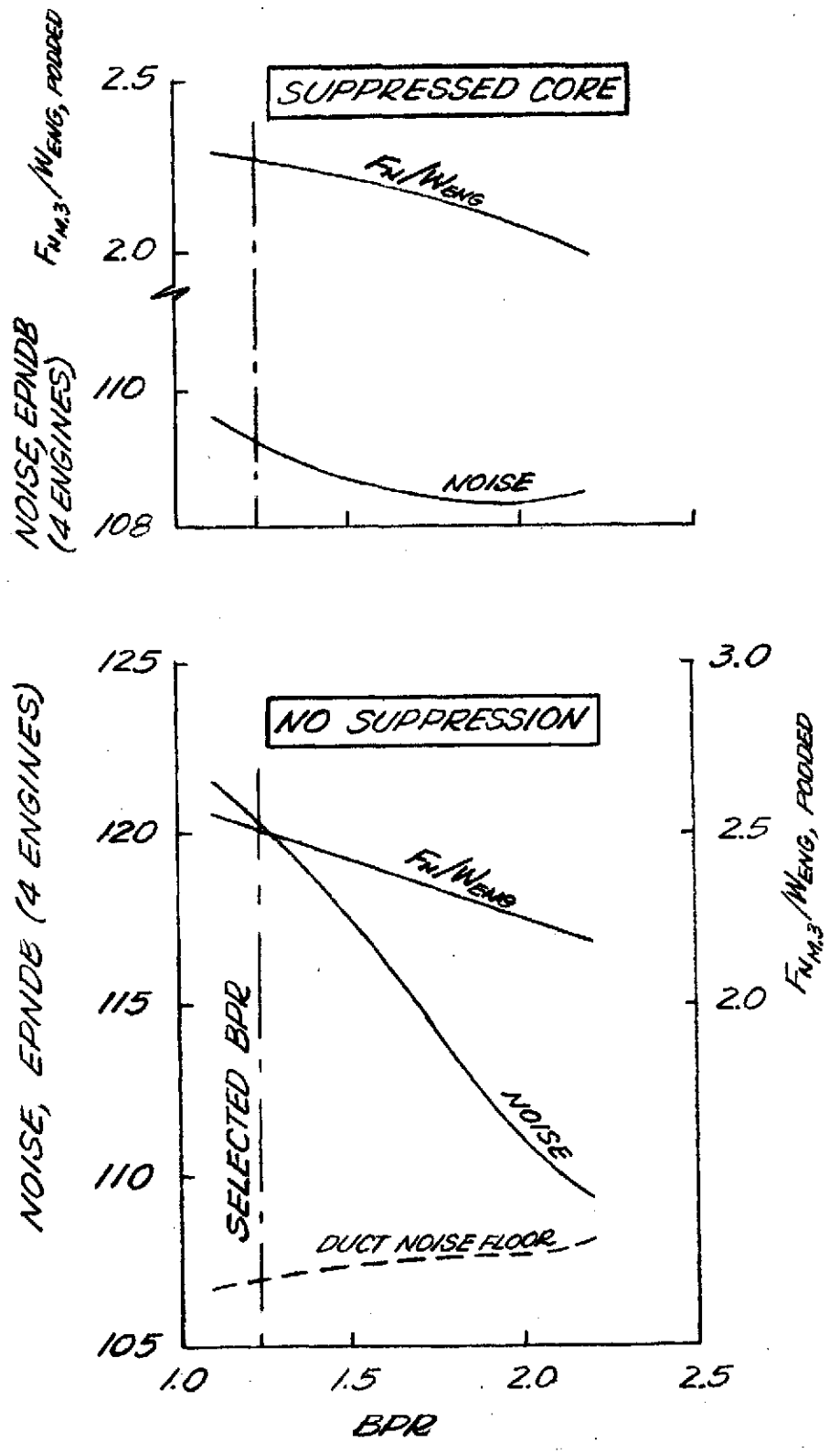

(A) FAN PRESSURE RATIO = 3.5

FIGURE 8. – EFFECT OF DESIGN BYPASS RATIO ON SIDELINE JET NOISE AND INSTALLED LIFT-OFF THRUST-WEIGHT RATIO FOR SEPARATE-FLOW TURBOFANS WITH 1000 LB/SEC

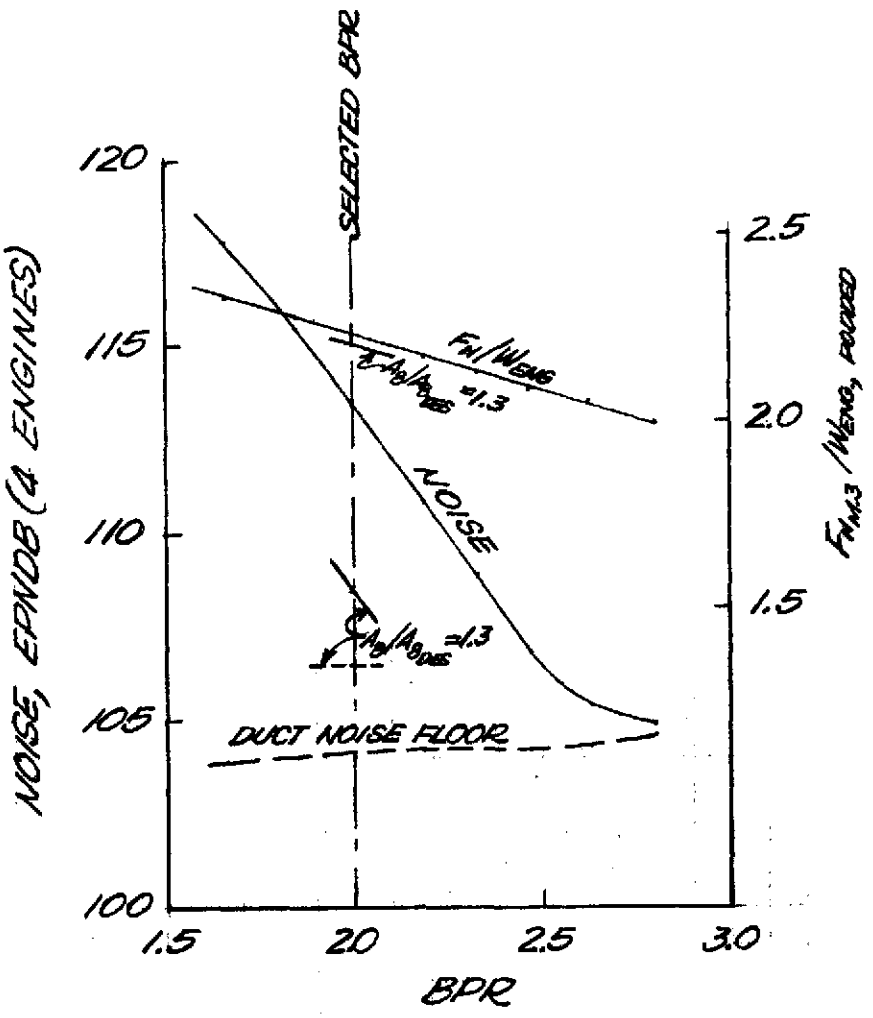

(B) FAN PRESSURE RATIO = 3.0. UNSUPPRESSED.

FIGURE 8.– CONTINUED.

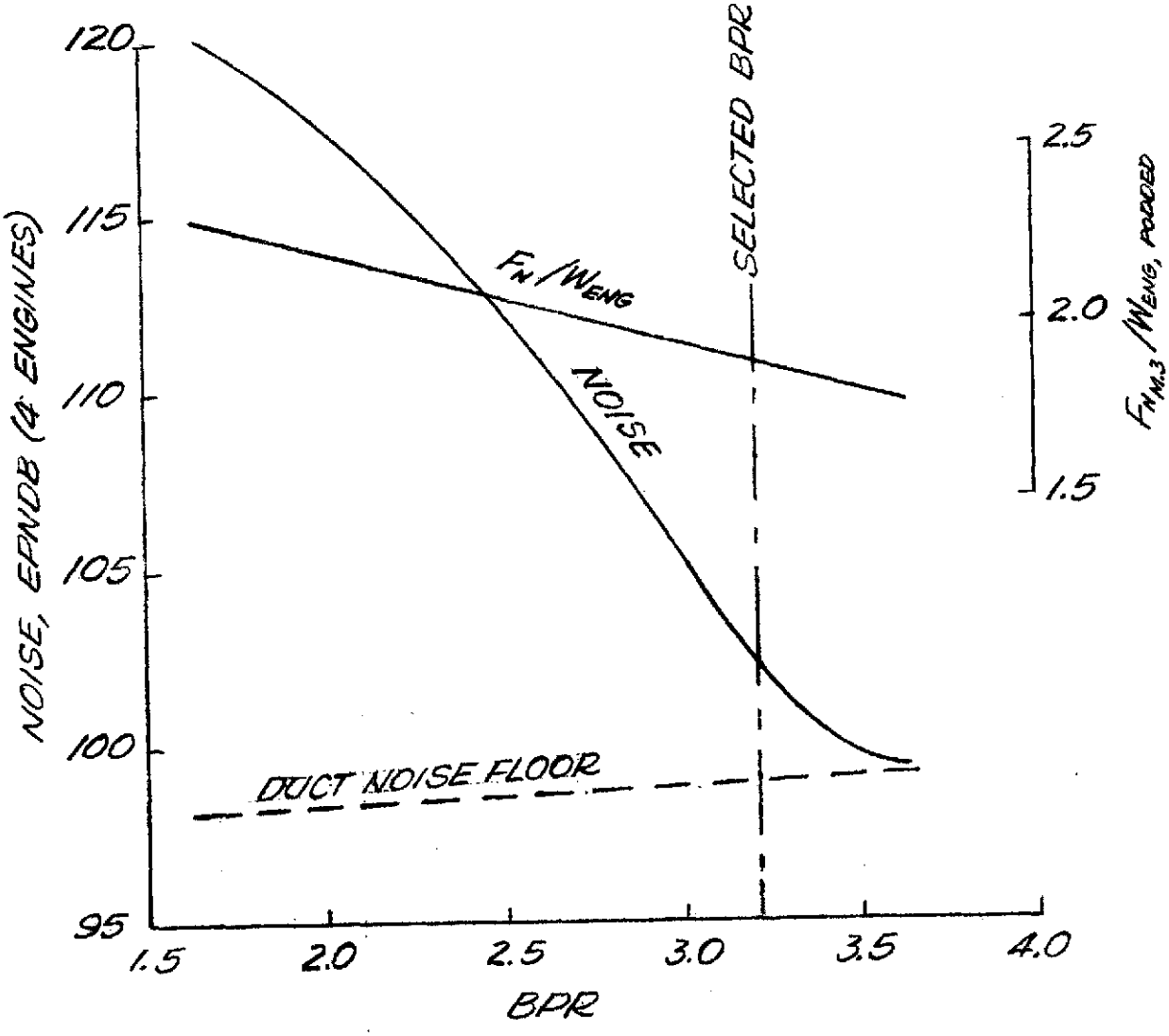

(C) FAN PRESSURE RATIO = 2.5. UNSUPPRESSED.

FIGURE 8. – CONTINUED.

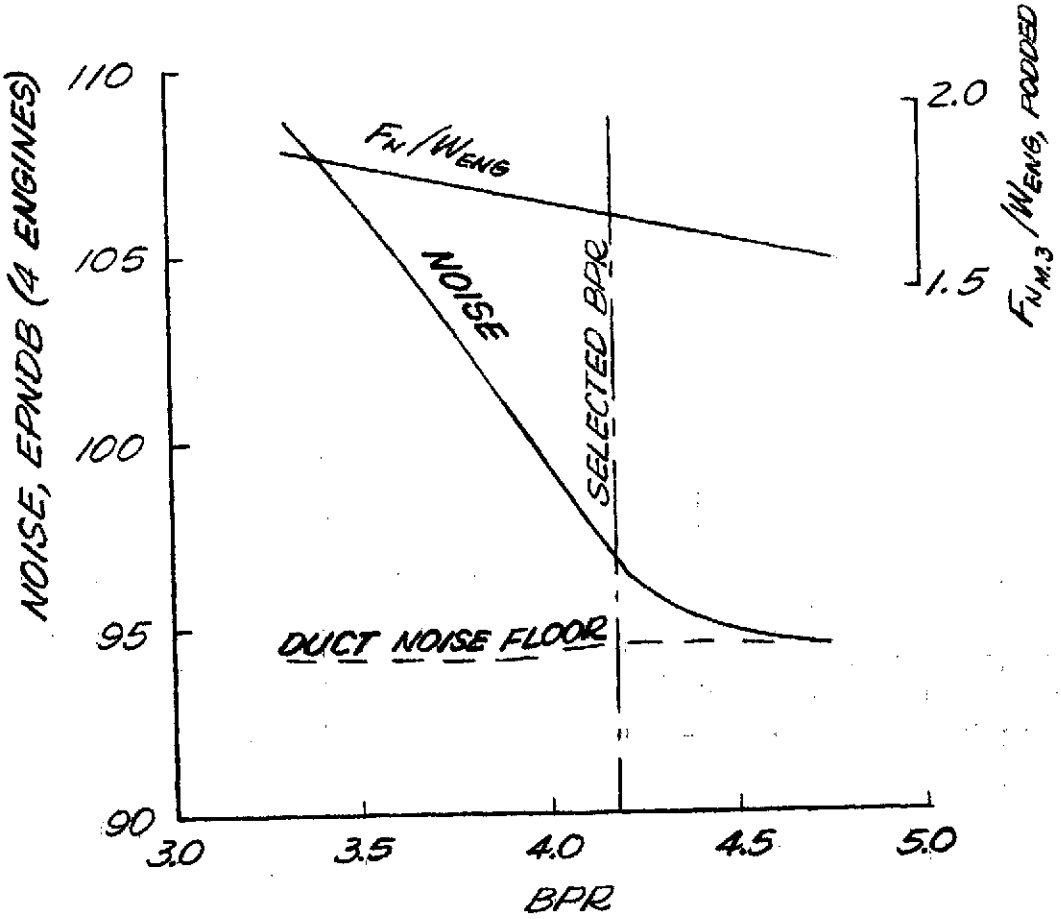

(D) FAN PRESSURE RATIO = 2.2. UNSUPPRESSED.

FIGURE 8. — CONCLUDED.

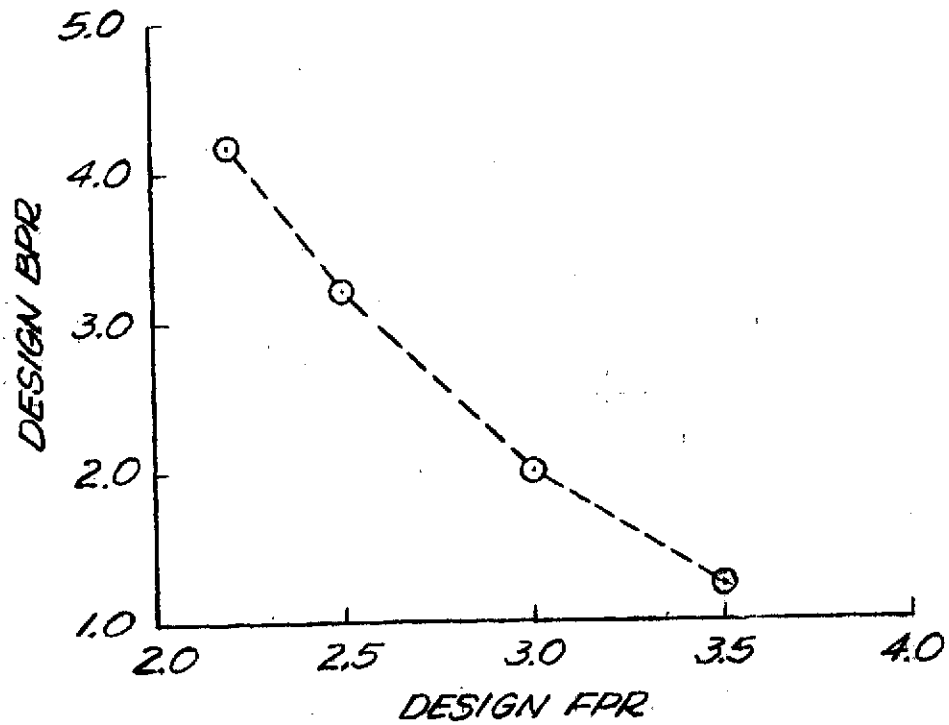

FIGURE 9. – SUMMARY OF BYPASS RATIOS SELECTED FOR THE FAN PRESSURE RATIO SPECTRUM CONSIDERED FOR DUCT-BURNING TURBOFAN ENGINES.

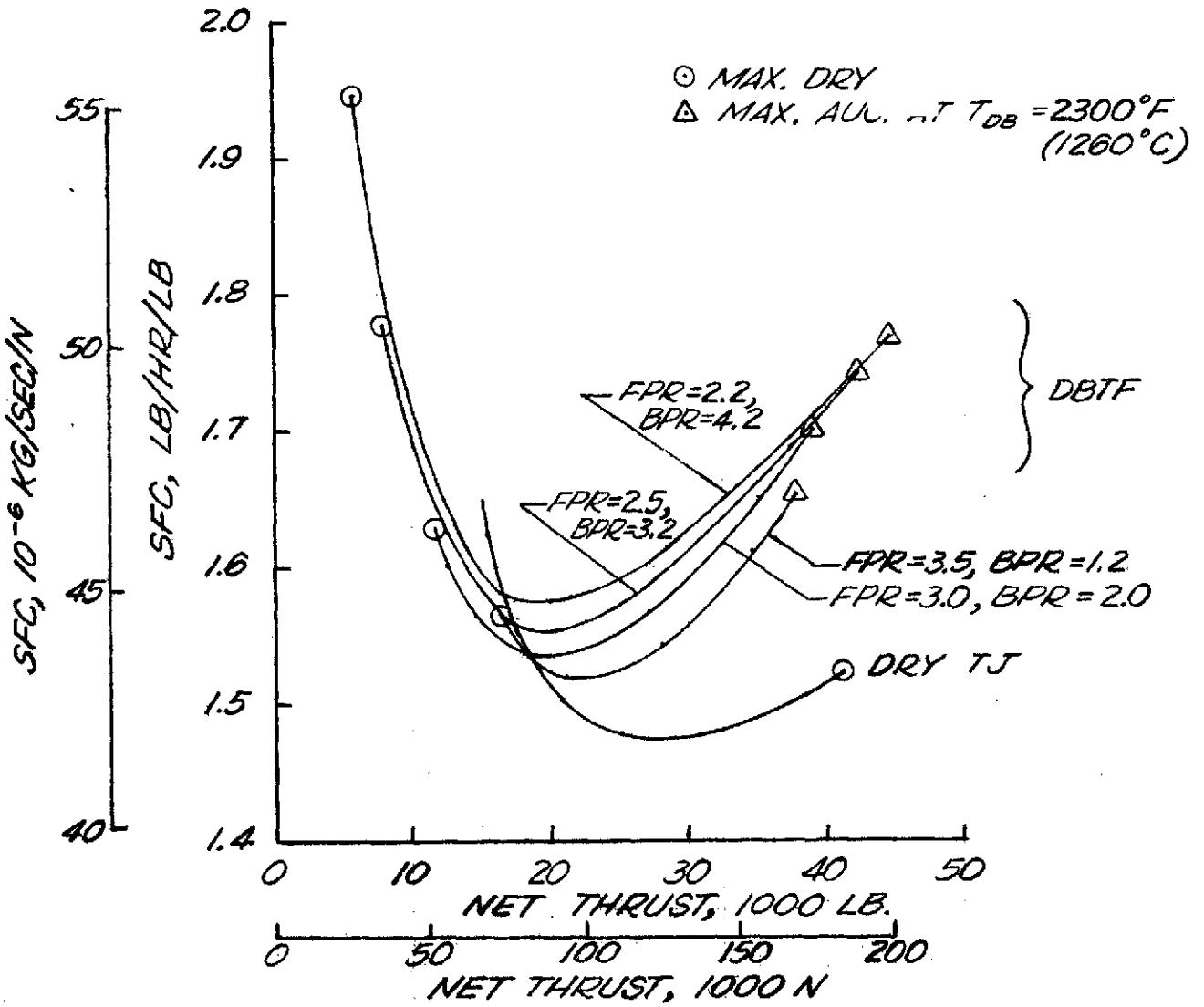

(A) MACH 2.7, ALTITUDE = 60 000 FT (18 288 M).

FIGURE 10 — INSTALLED CRUISE PERFORMANCE COMPARISON OF STUDY ENGINES. DESIGN AIRFLOW=1000 LB/SEC (454 KG/SEC).

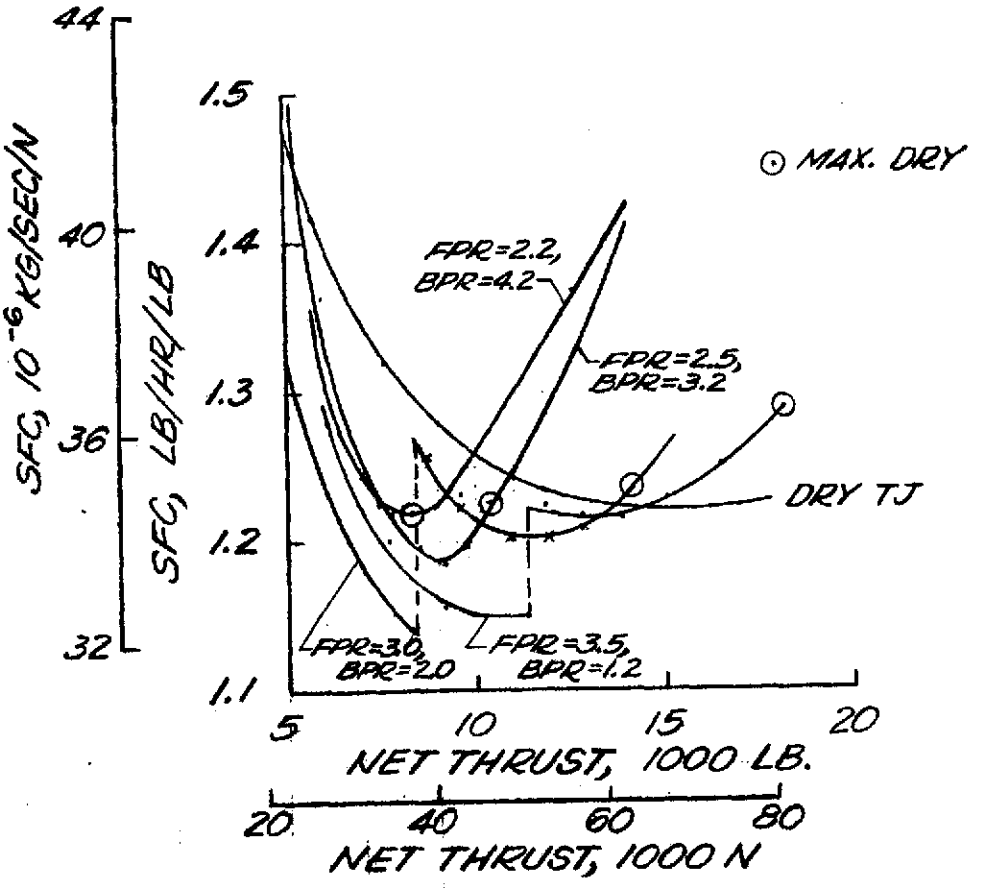

(B) MACH 0.95, ALTITUDE = 36 089 FT (11 000 M)

FIGURE 10.– CONCLUDED.

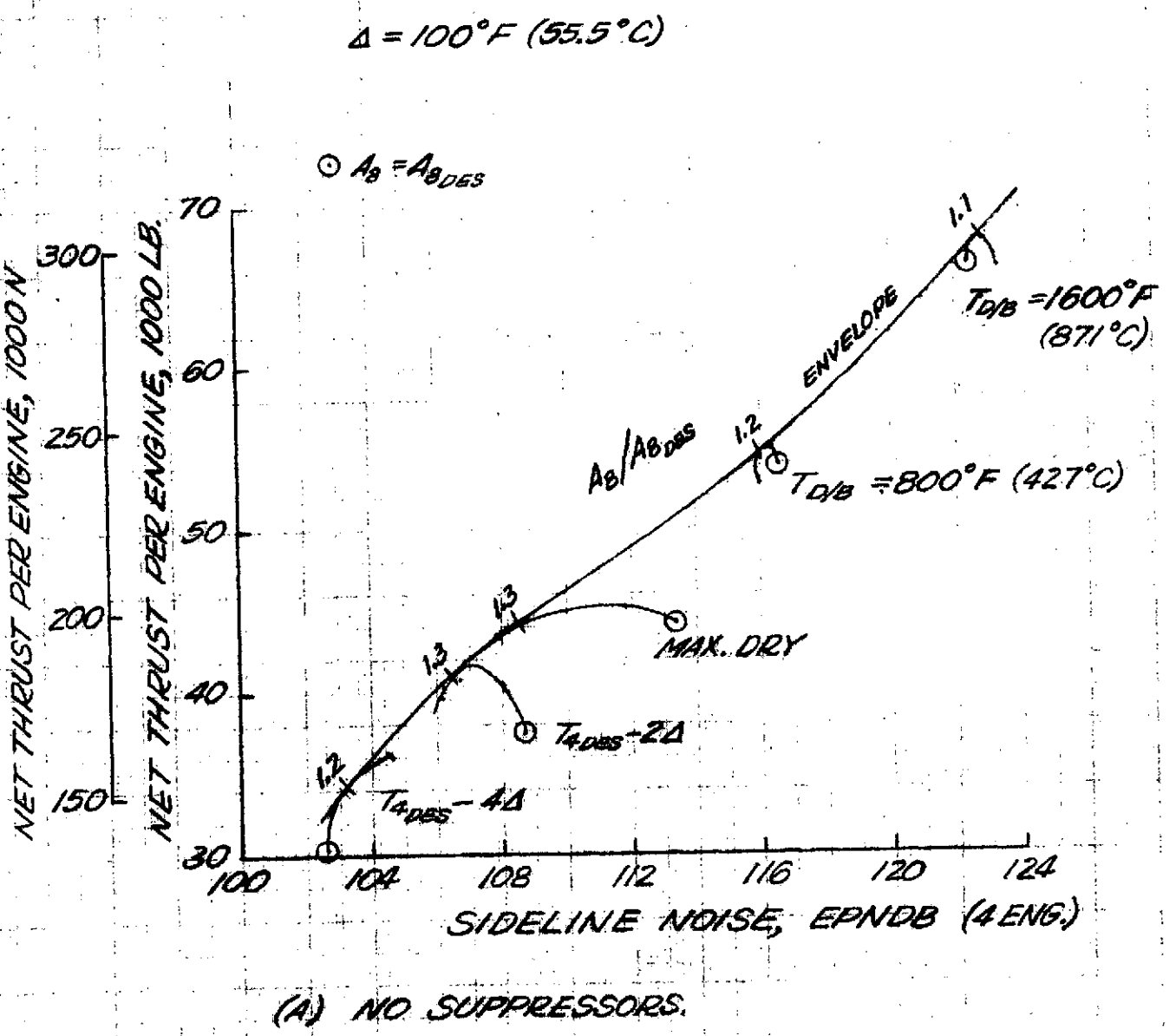

(A) NO SUPPRESSORS.

FIGURE 11. – OPTIMIZATION OF TURBOFAN ENGINE COMPONENT MATCHING AT MACH 0.3 LIFT-OFF CONDITION BY VARIATION OF CORE NOZZLE THROAT AREA A_8. DESIGN AIRFLOW=1000 LB/SEC (454 KG/SEC). DESIGN T_4 =2725°F (1496°C). FPR=3.0, BPR=2.0.

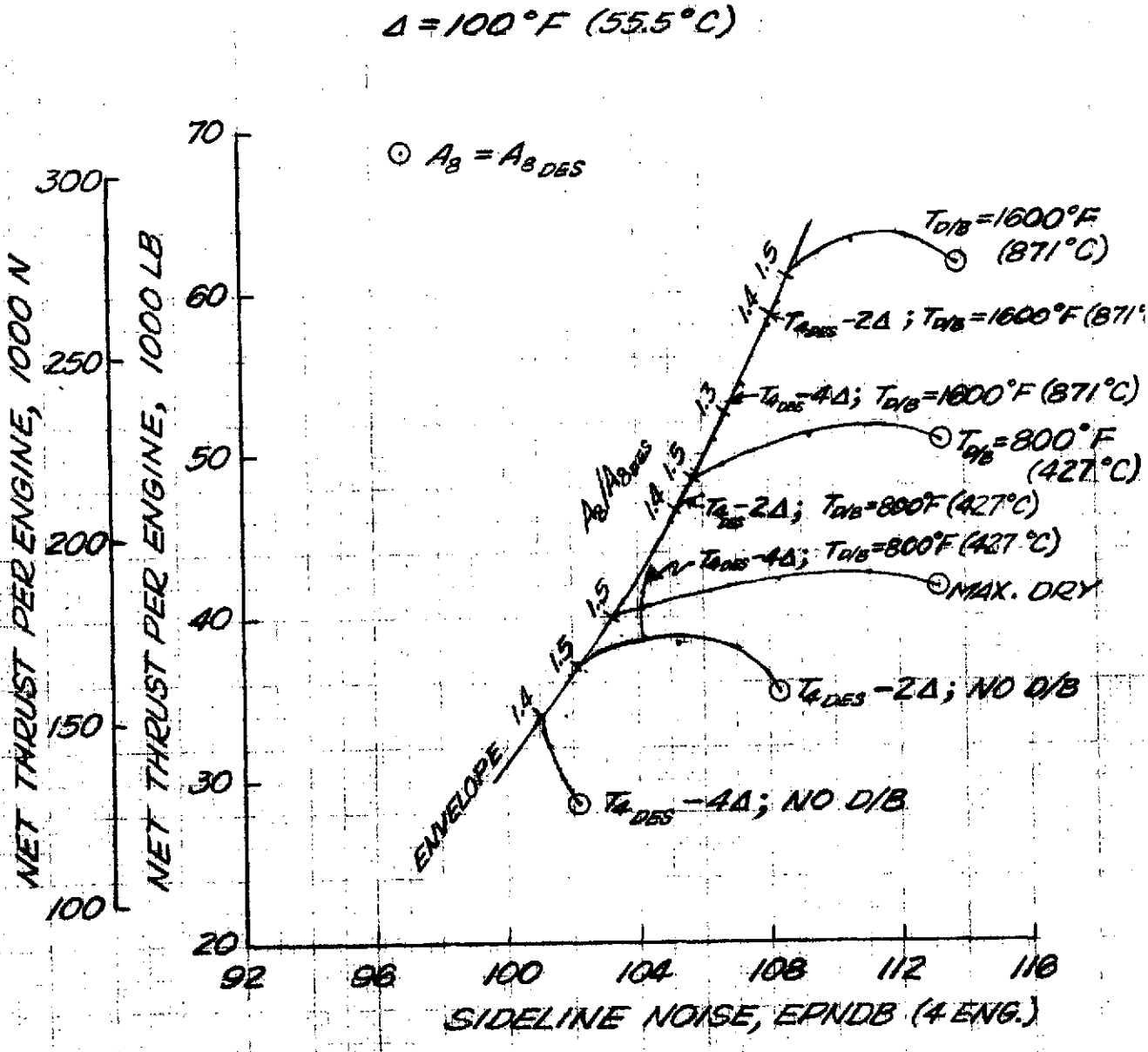

(B) DUCT SUPPRESSOR ONLY.

FIGURE 11. - CONTINUED.

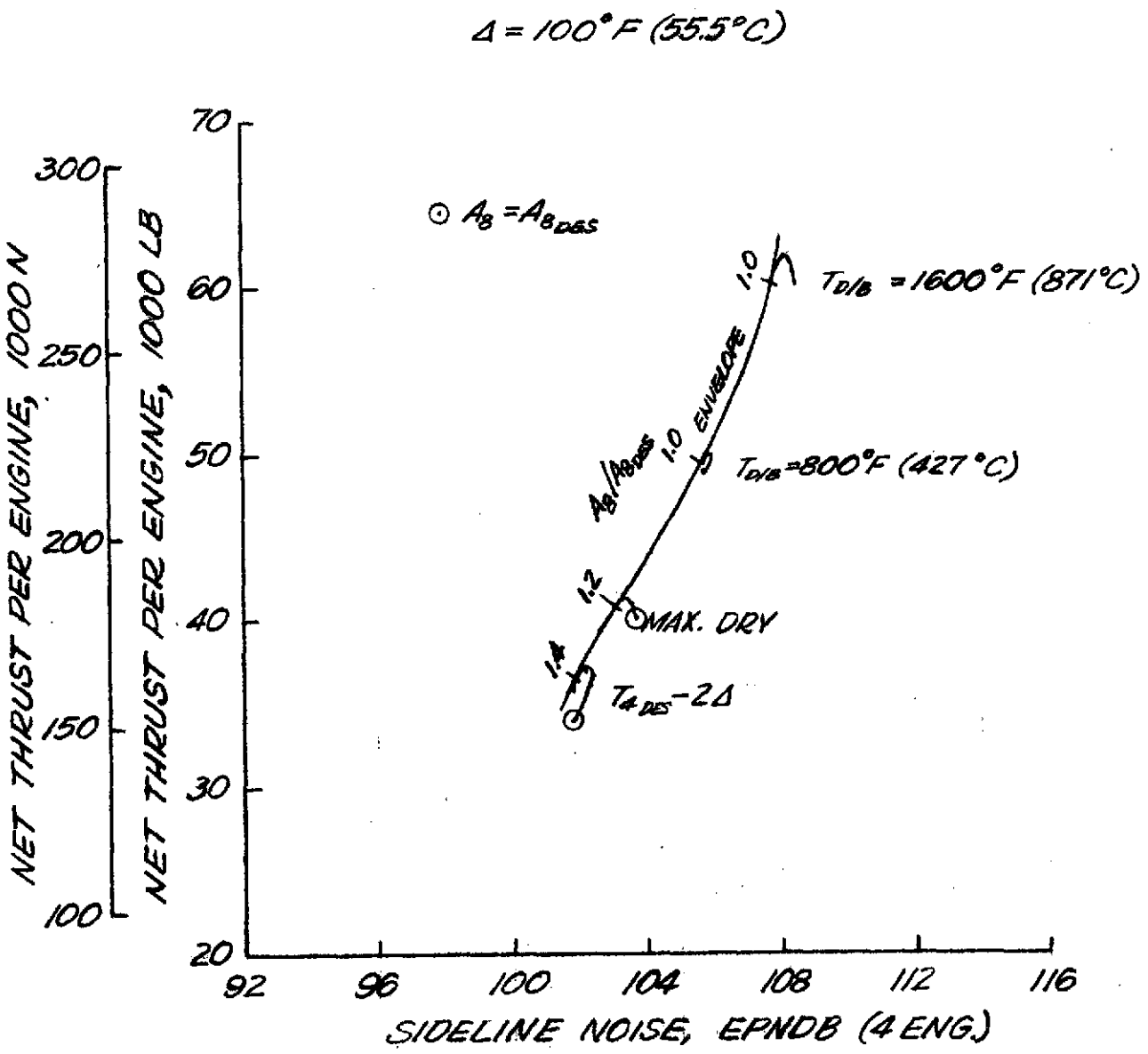

(C) BOTH DUCT AND CORE SUPPRESSORS.

FIGURE 11. – CONCLUDED.

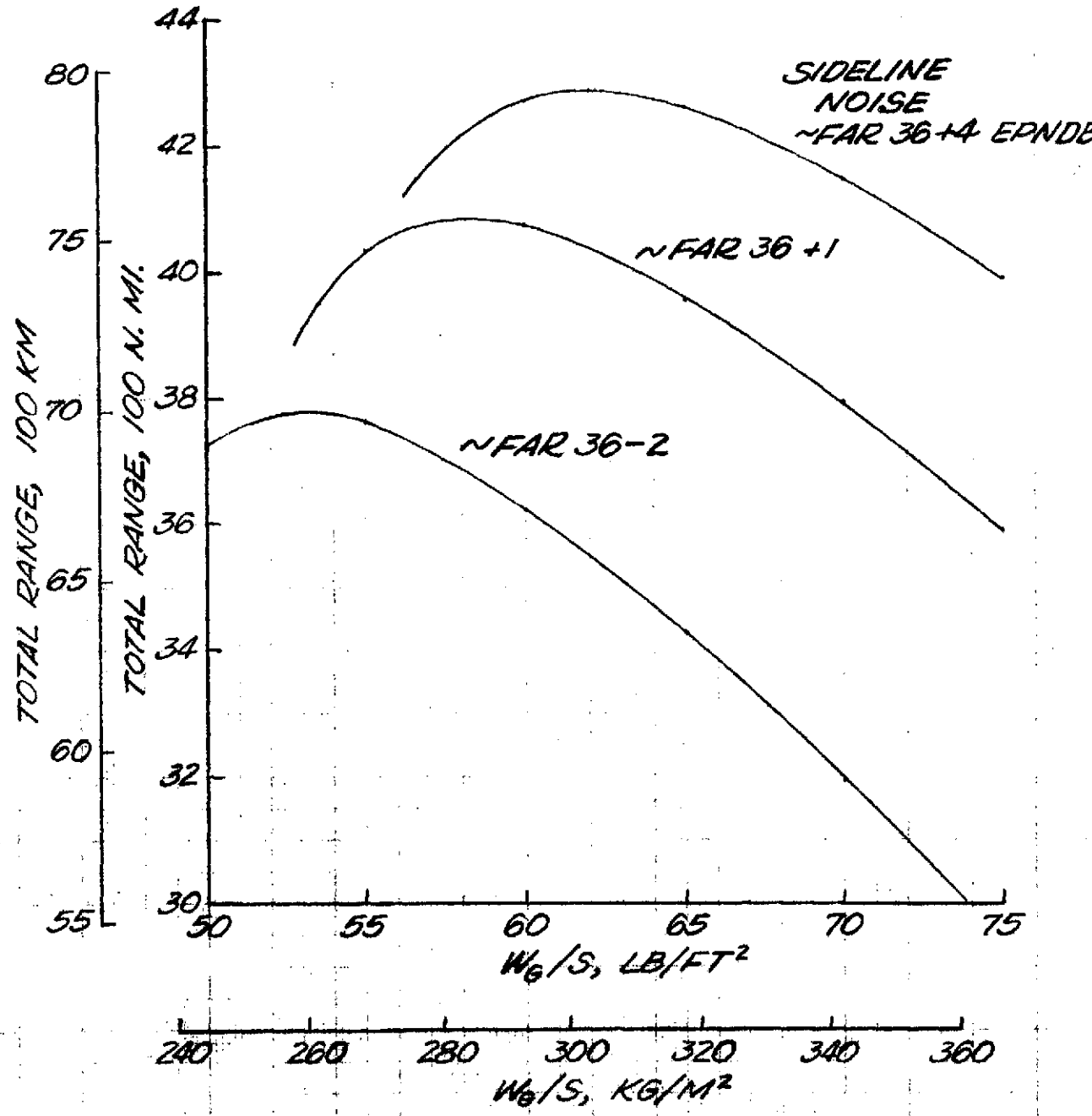

FIGURE 12.- EFFECT OF SIDELINE NOISE LEVEL ON OPTIMUM WING LOADING FOR SUPPRESSED DRY TURBOJETS. TAKEOFF GROSS WEIGHT = 750 000 LB (340 200 KG); 600 N MI (1111 KM) INITIALLY SUBSONIC. FAR T.O.F.L. = 10 500 FT (3200 M).

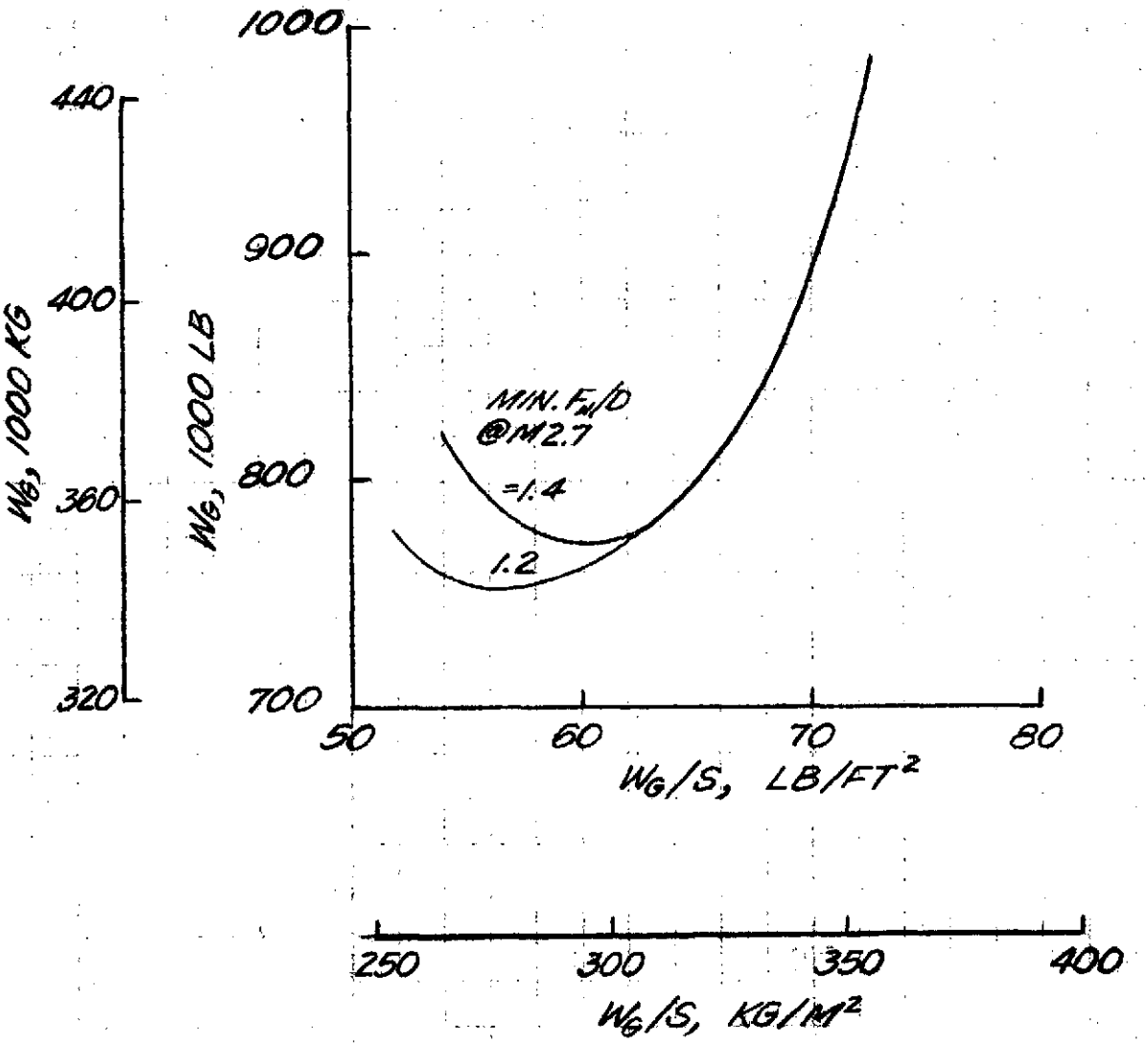

FIGURE 13. – EFFECT OF MINIMUM CLIMB/ACCEL THRUST-DRAG RATIO ON OPTIMUM WING LOADING AND MINIMUM GROSS WEIGHT FOR SUPPRESSED DRY TURBOJETS AT FAR 36 SIDELINE NOISE. FAR TAKEOFF FIELD LENGTH = 10 500 FT (3200 M). 4000 N MI (7408 KM) TOTAL RANGE WITH FIRST 600 N MI (1111 KM) SUBSONIC.

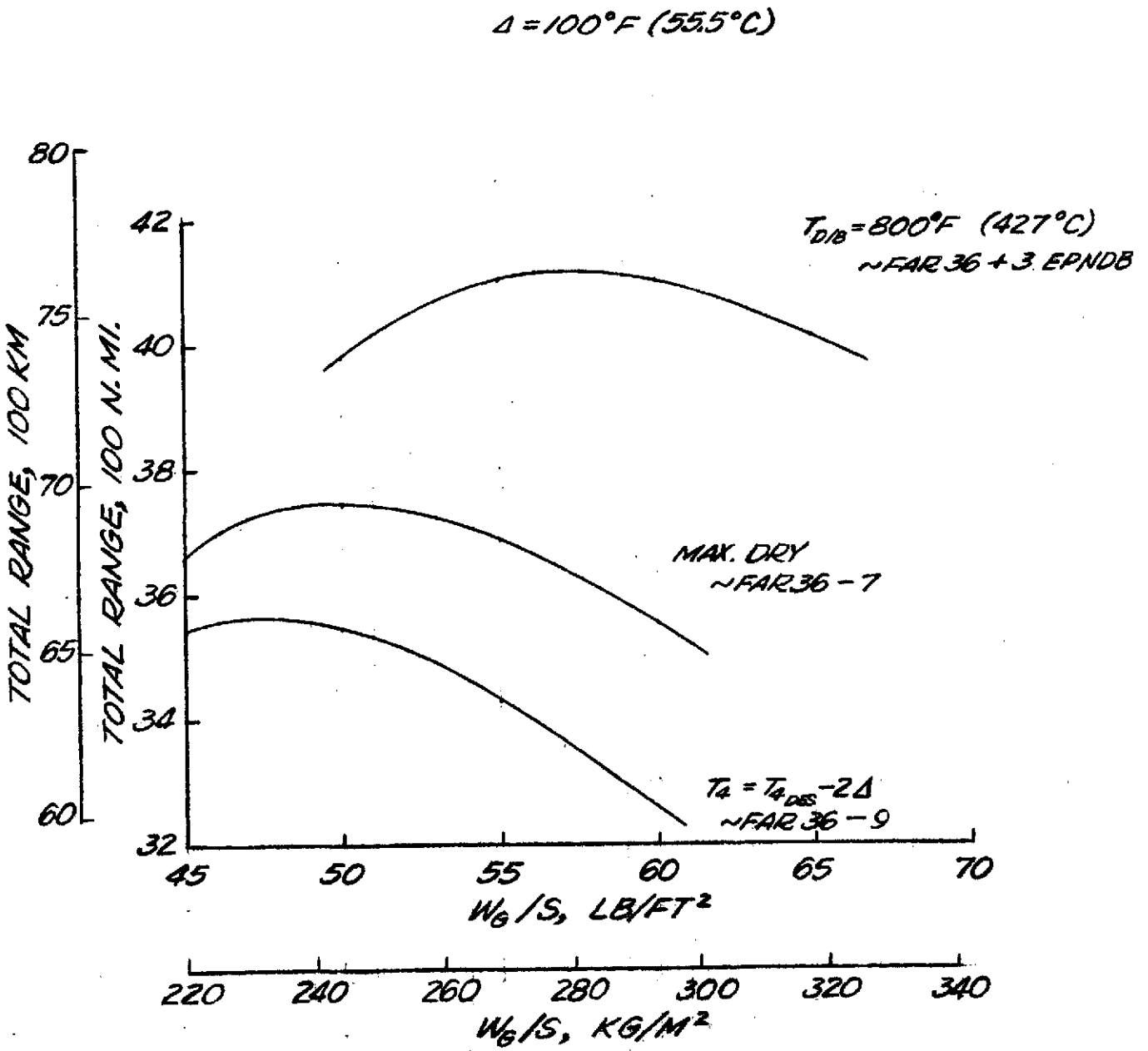

(A) NO SUPPRESSORS.

FIGURE 14. – EFFECT OF SIDELINE NOISE LEVEL ON OPTIMUM WING LOADING FOR DUCT-BURNING TURBOFANS WITH FPR = 2.5 AND BPR = 3.21. TAKEOFF GROSS WEIGHT = 700 000 LB (317 744 KG). FIRST 600 N MI (1111 KM) SUBSONIC. FAR T.O.F.L. = 10 500 FT (3200 M).

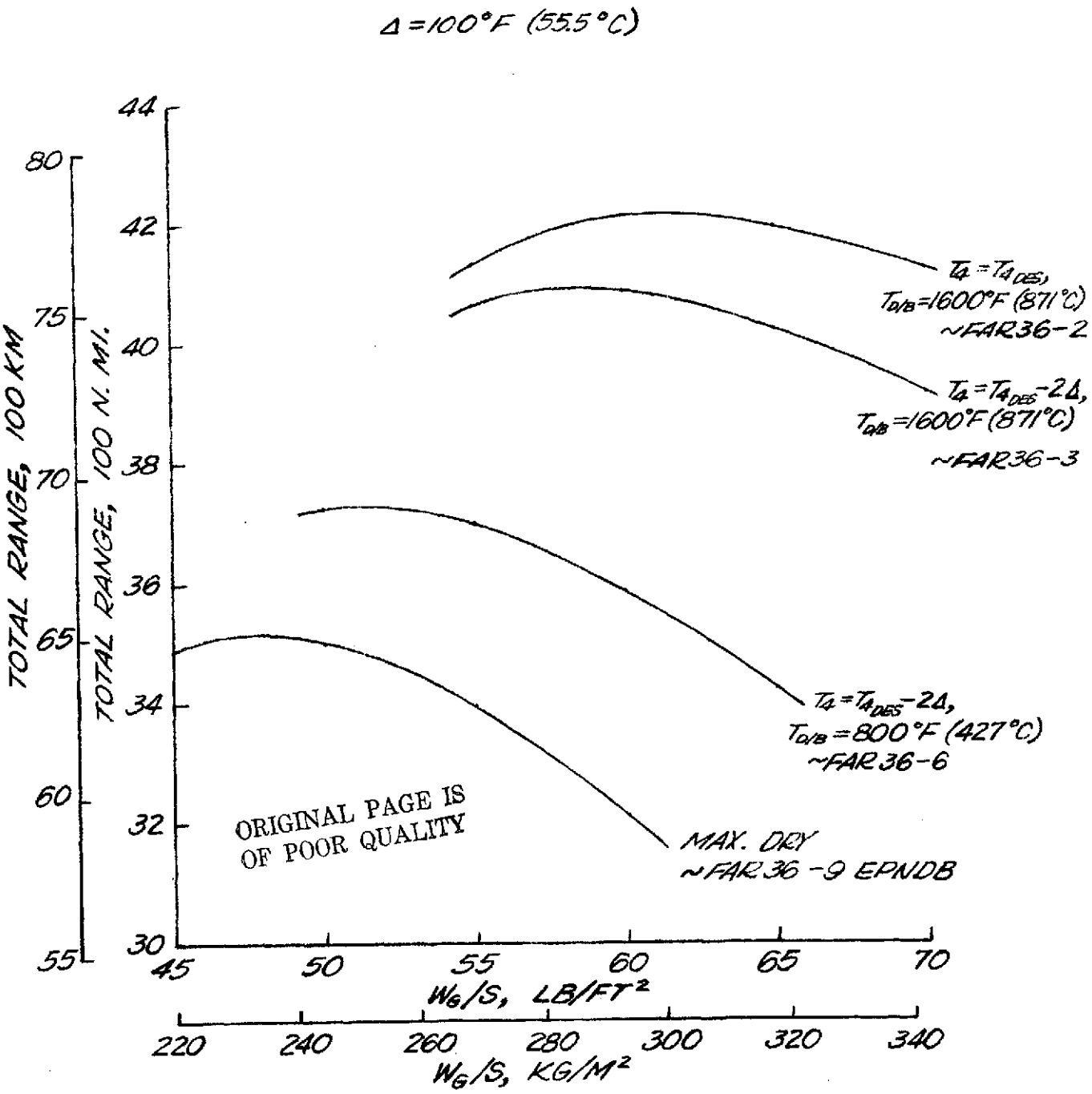

(B) DUCT SUPPRESSOR ONLY.

FIGURE 14. – CONCLUDED.

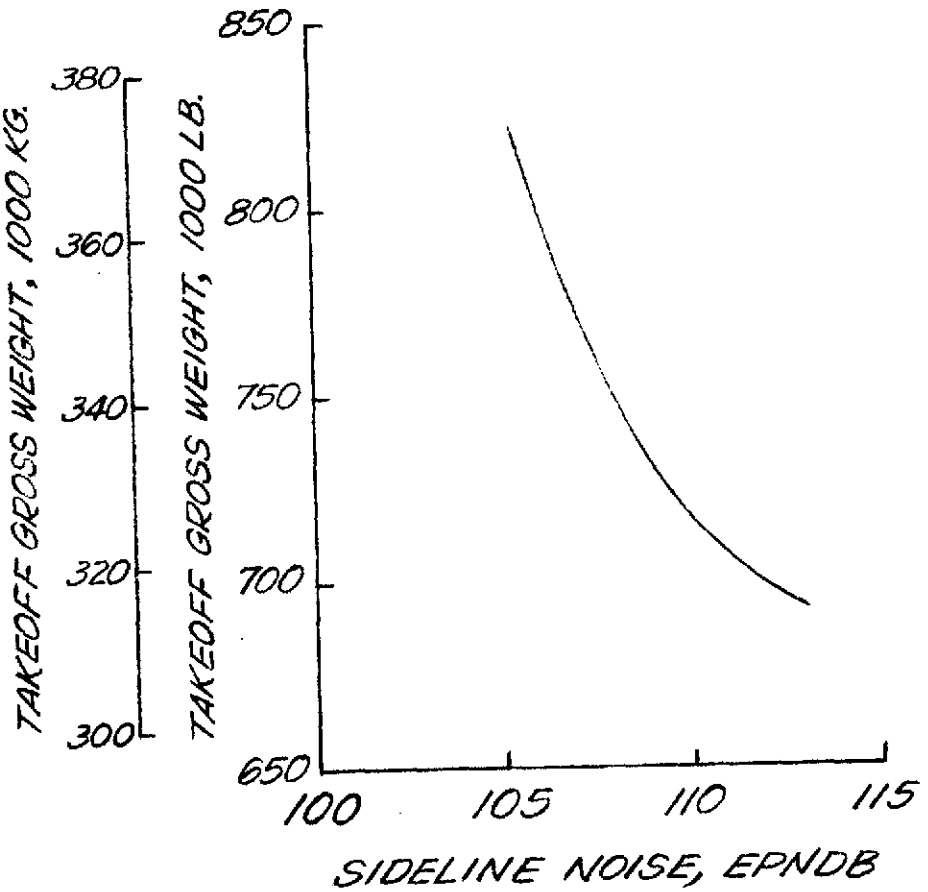

FIGURE 15. – EFFECT OF SIDELINE NOISE ON GROSS WEIGHT WITH SUPPRESSED NON-AFTERBURNING TURBOJETS. TOTAL RANGE = 4000 N MI (7408 KM); FIRST 600 N MI (1111 KM) SUBSONIC. FAR TAKEOFF FIELD LENGTH = 10 500 FT (3200 M). WING LOADING OPTIMIZED.

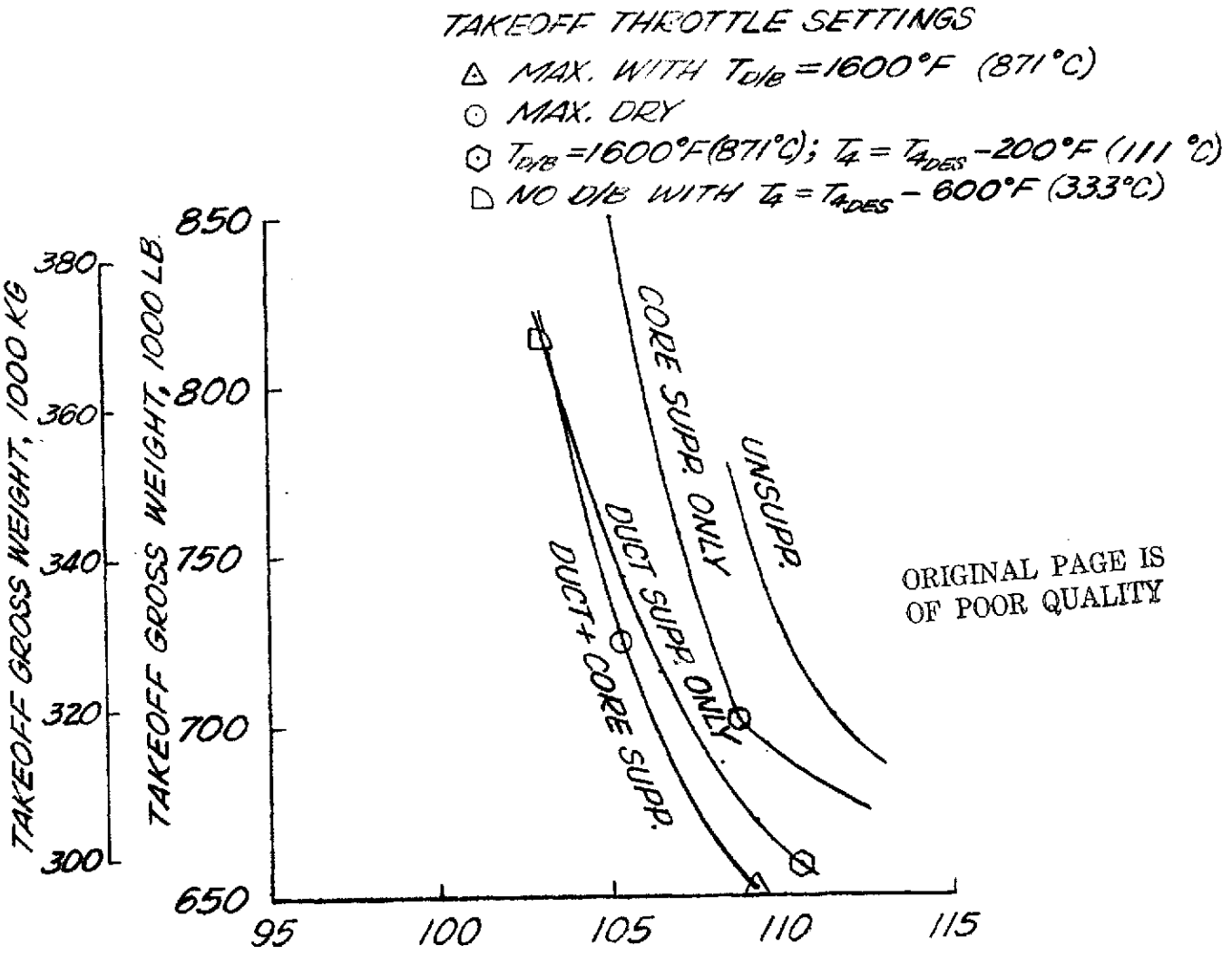

(A) FAN PRESSURE RATIO = 3.5, BYPASS RATIO = 1.23.

FIGURE 16. – EFFECT OF SIDELINE NOISE ON GROSS WEIGHT WITH DUCT-BURNING TURBOFAN ENGINES. TOTAL RANGE = 4000 N. MI. (7408 KM); FIRST 600 N. MI (1111 KM) SUBSONIC. FAR TAKEOFF FIELD LENGTH = 10 500 FT (3200 M). WING LOADING OPTIMIZED.

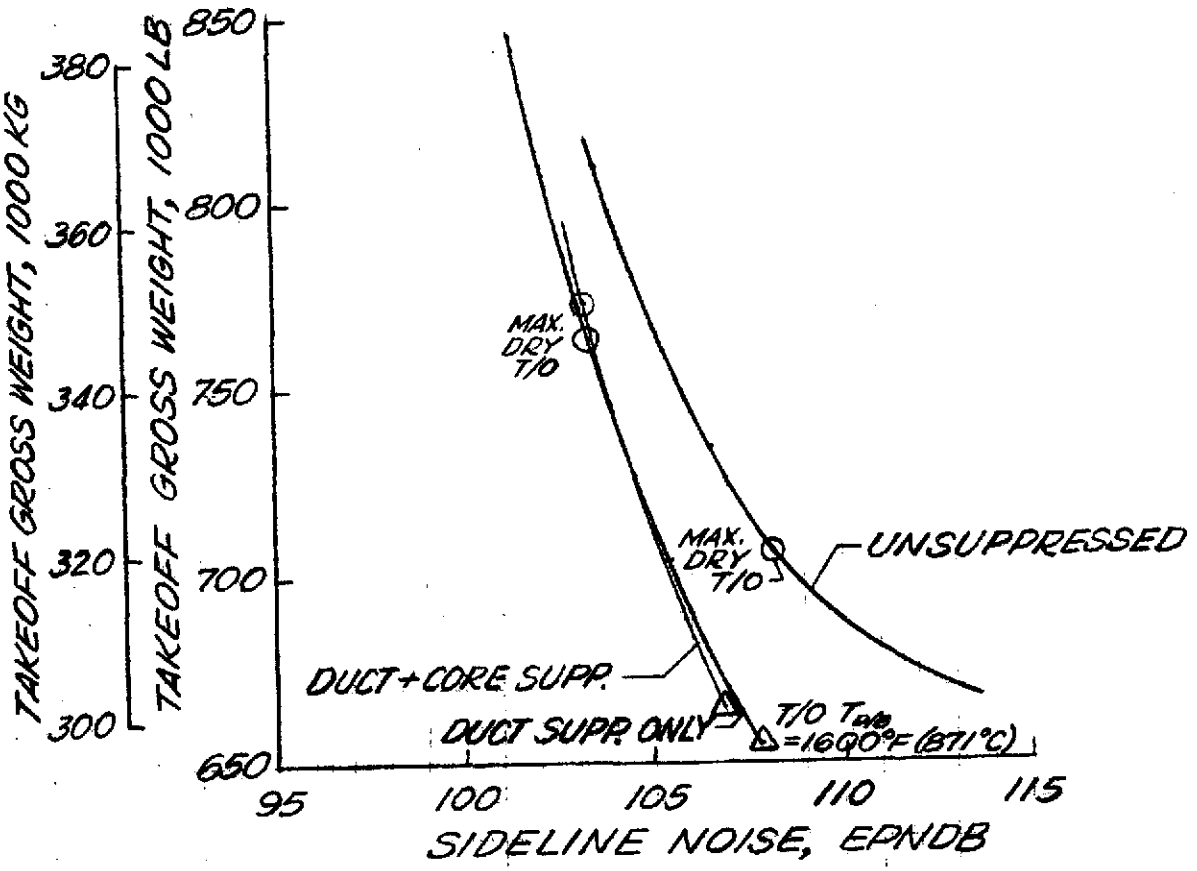

(B) FAN PRESSURE RATIO = 3.0, BYPASS RATIO = 2.00.

FIGURE 16. — CONTINUED.

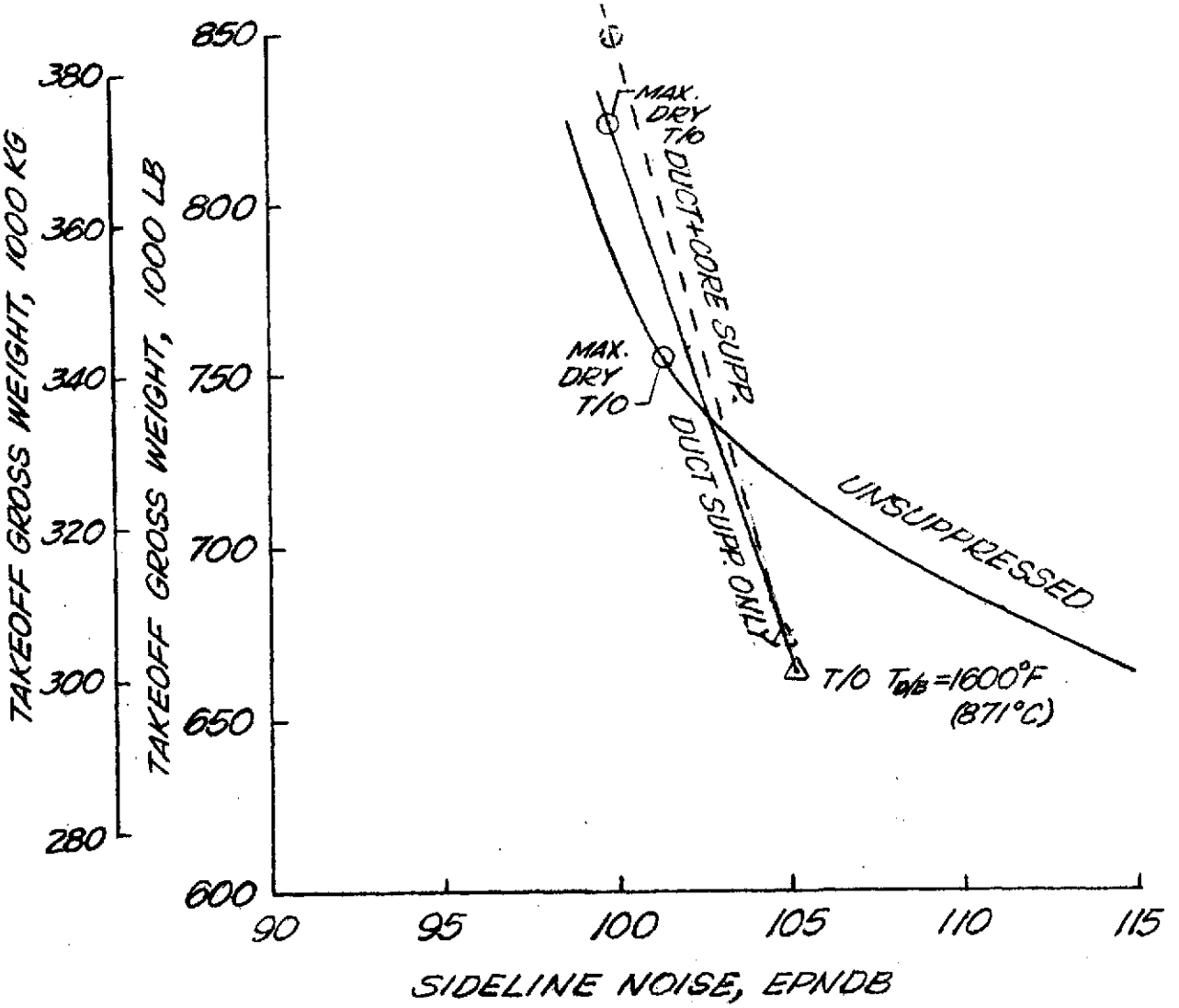

(C) FAN PRESSURE RATIO = 2.5, BYPASS RATIO = 3.21.

FIGURE 16. – CONCLUDED.

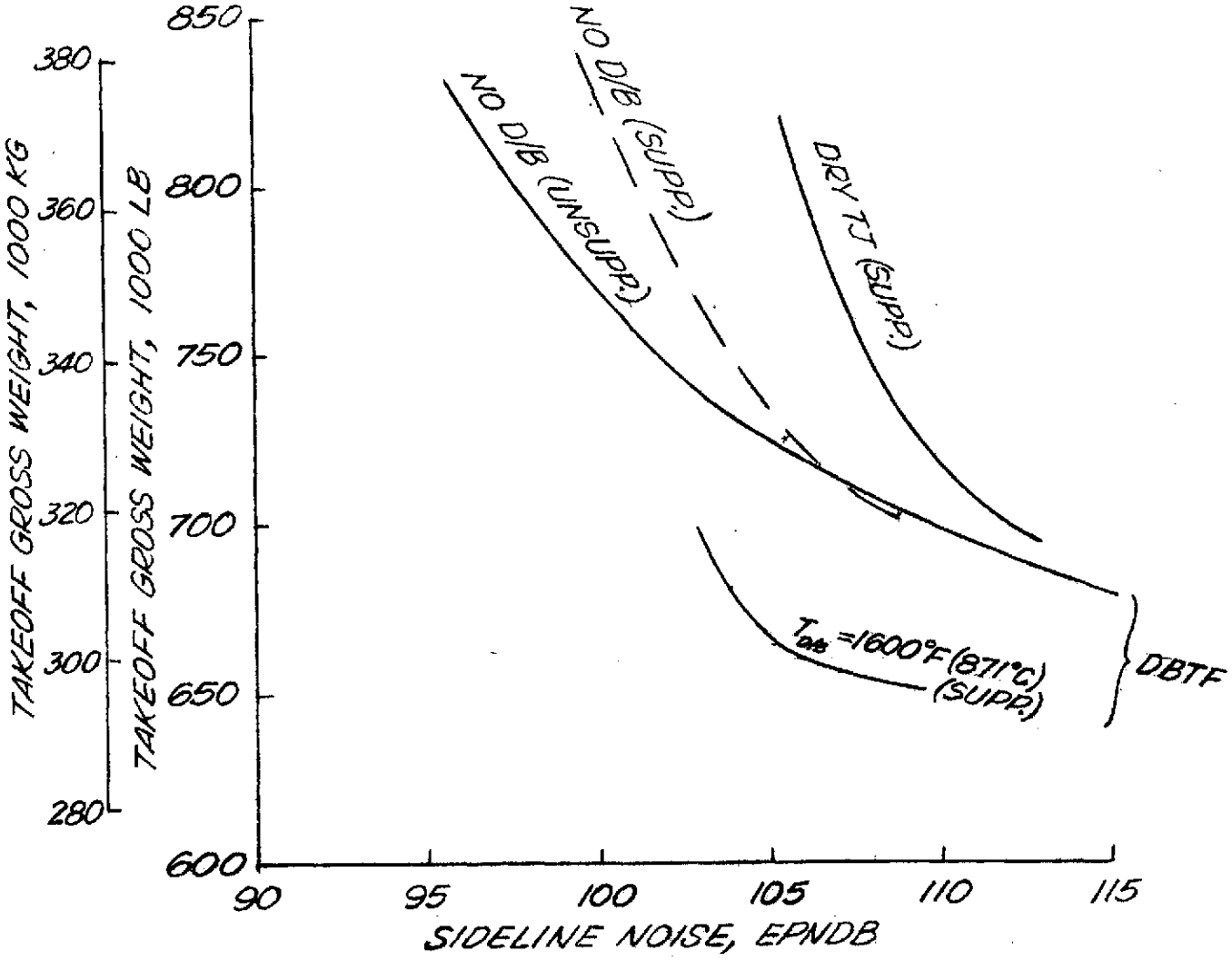

(A) TAKEOFF GROSS WEIGHT

FIGURE 17. – COMPARISON OF BEST ENGINE CYCLES OVER A RANGE OF SIDELINE NOISE. TOTAL RANGE = 4000 N MI (7408 KM); FIRST 600 N MI (1111 KM) SUBSONIC. FAR T.O.F.L. = 10 500 FT (3200 M). WING LOADING OPTIMIZED.

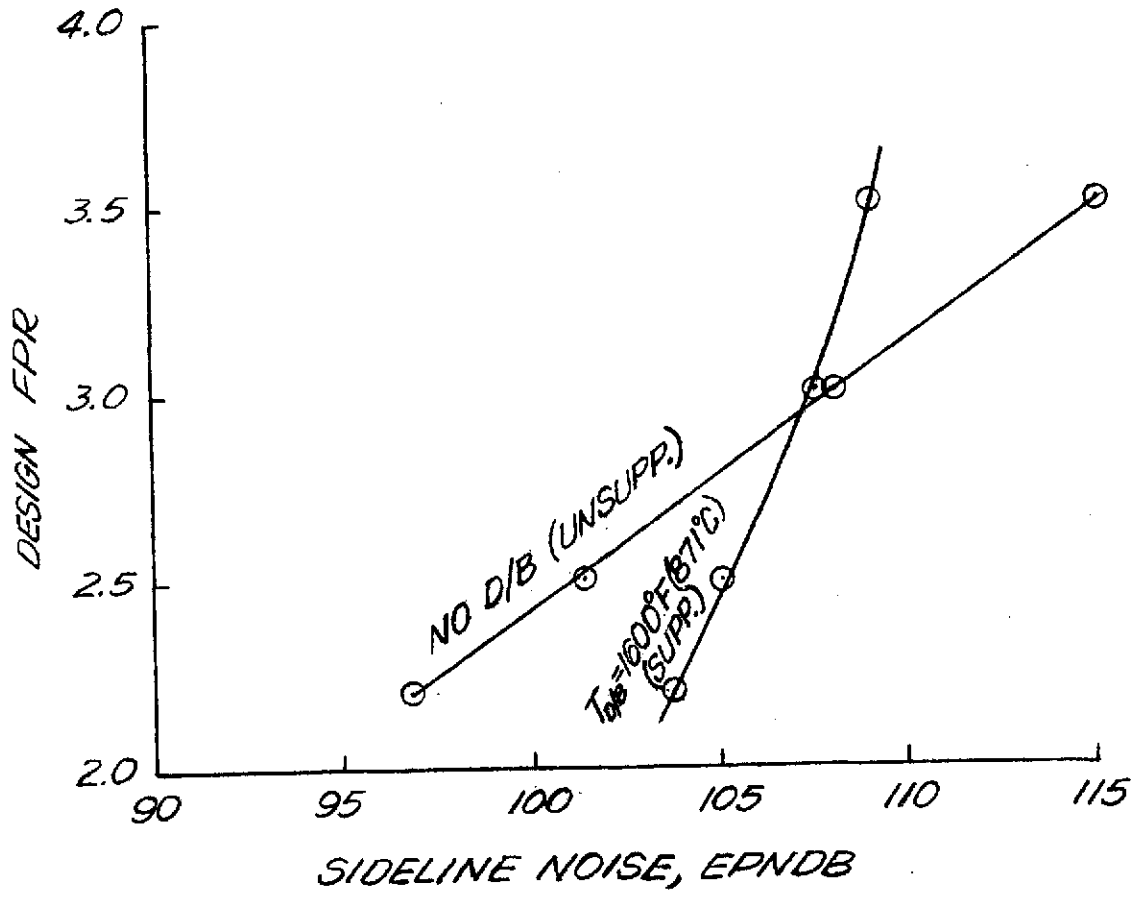

(B) FAN PRESSURE RATIO OF DUCT-BURNING TURBOFAN CYCLES.

FIGURE 17.– CONTINUED.

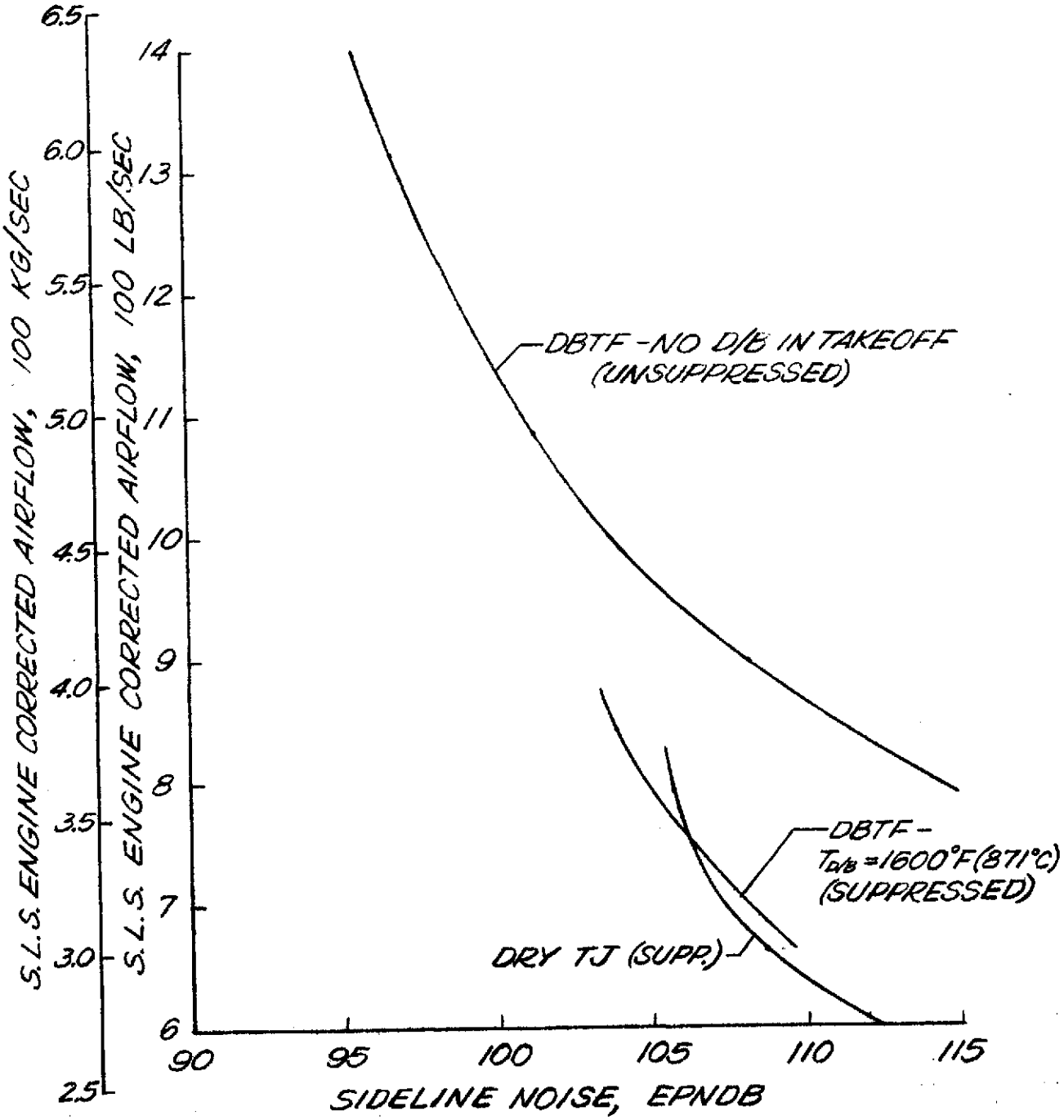

(C) SEA-LEVEL-STATIC DESIGN CORRECTED AIRFLOW PER ENGINE.

FIGURE 17. - CONCLUDED.

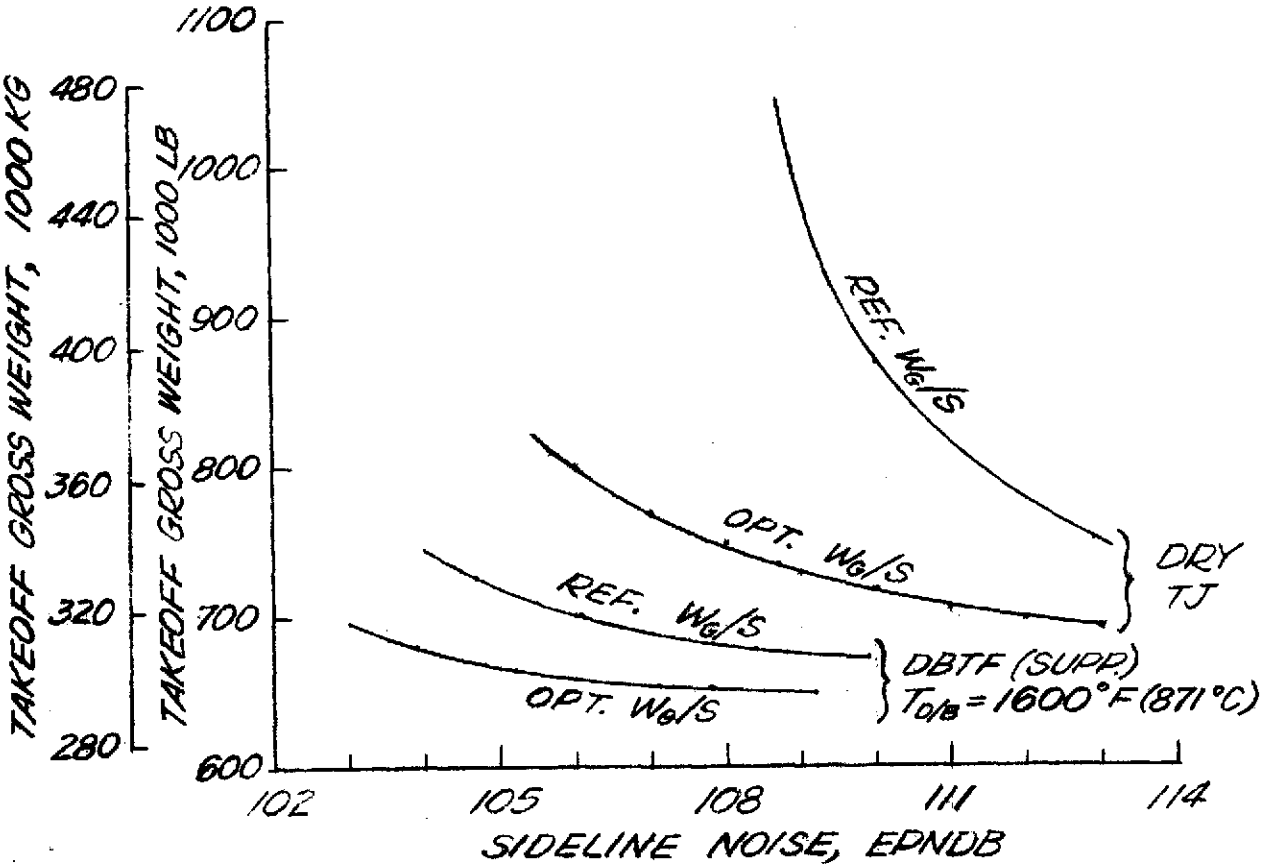

FIGURE 18. – BENEFIT RECEIVED FROM WING LOADING OPTIMIZATION INCORPORATED IN PRECEDING RESULTS. TOTAL RANGE = 4000 N MI (7408 KM); FIRST 600 N MI (1111 KM) SUBSONIC. FAR TAKEOFF FIELD LENGTH = 10 500 FT (3200 M).

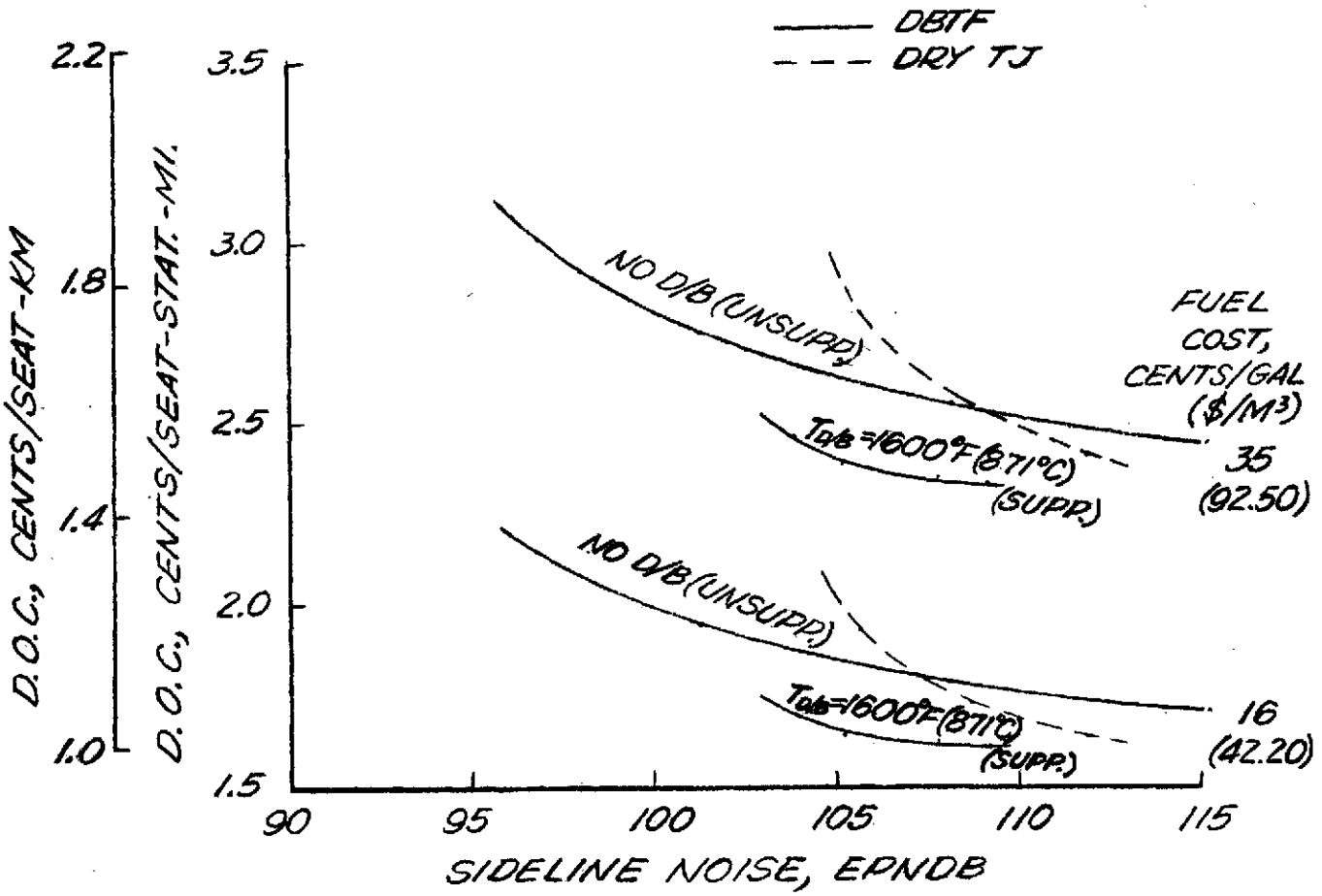

FIGURE 19 – COMPARISON OF AIRPLANE DIRECT OPERATING COSTS FOR TURBOJETS AND BEST DUCT-BURNING TURBOFAN ENGINE CYCLES OVER A RANGE OF SIDELINE NOISE. TOTAL RANGE = 4000 N. MI (7408 KM); FIRST 600 N. MI (1111 KM) SUBSONIC. FAR T.O.F.L. = 10 500 FT (3200 M). WING LOADING OPTIMIZED. 234 SEATS.

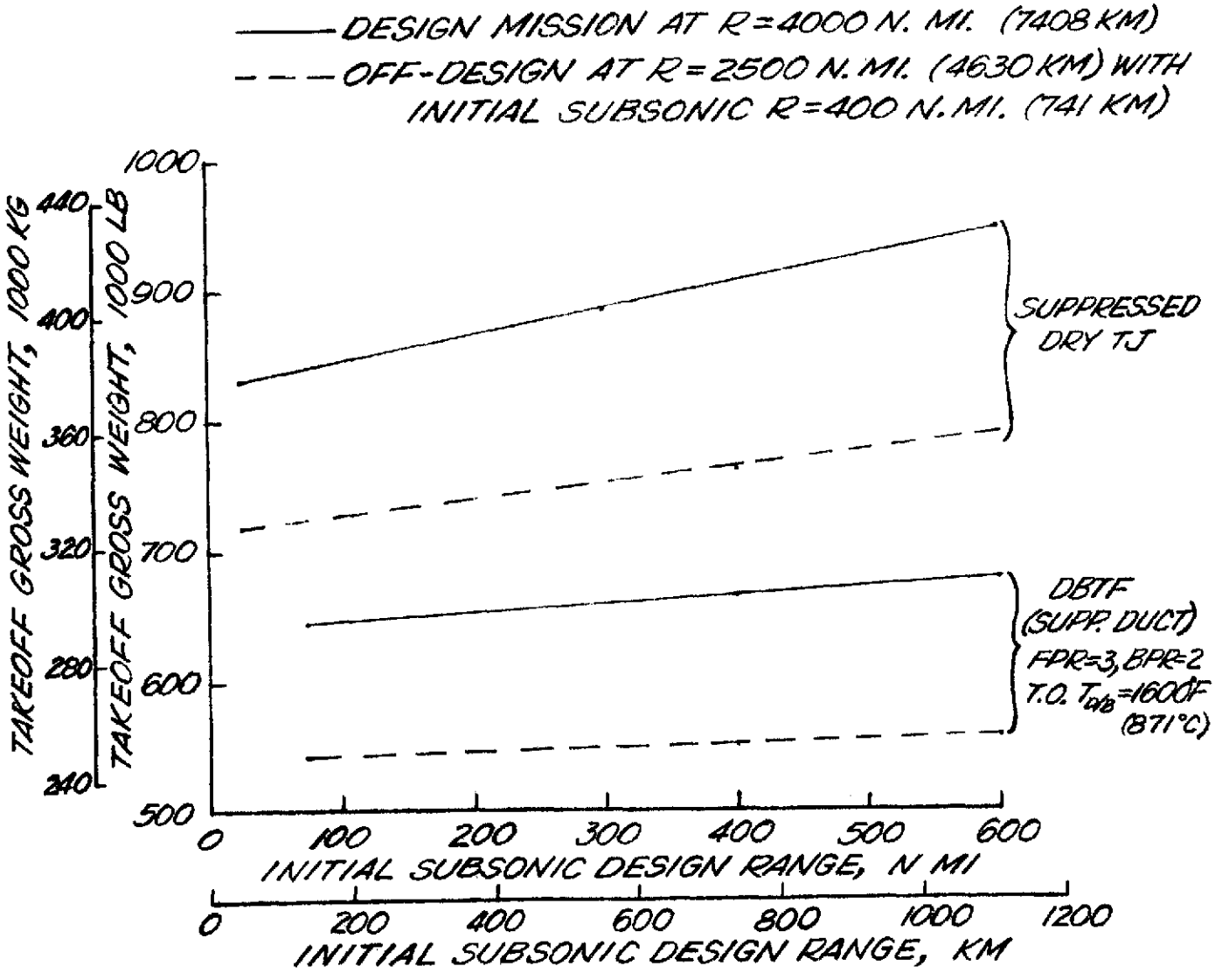

(A) TAKEOFF GROSS WEIGHT.

FIGURE 20. – EFFECT OF INITIAL SUBSONIC DESIGN RANGE ON MISSION RESULTS FOR DESIGN MISSION AND AVERAGE OFF-DESIGN MISSION (REF. 17) FOR TWO DIFFERENT ENGINE CYCLES. REFERENCE 75 LB/FT² (366 KG/M²) WING LOADING. FAR T. O. F. L. = 10 500 FT (3200 M). FAR 36 +1 EPNDB SIDELINE NOISE.

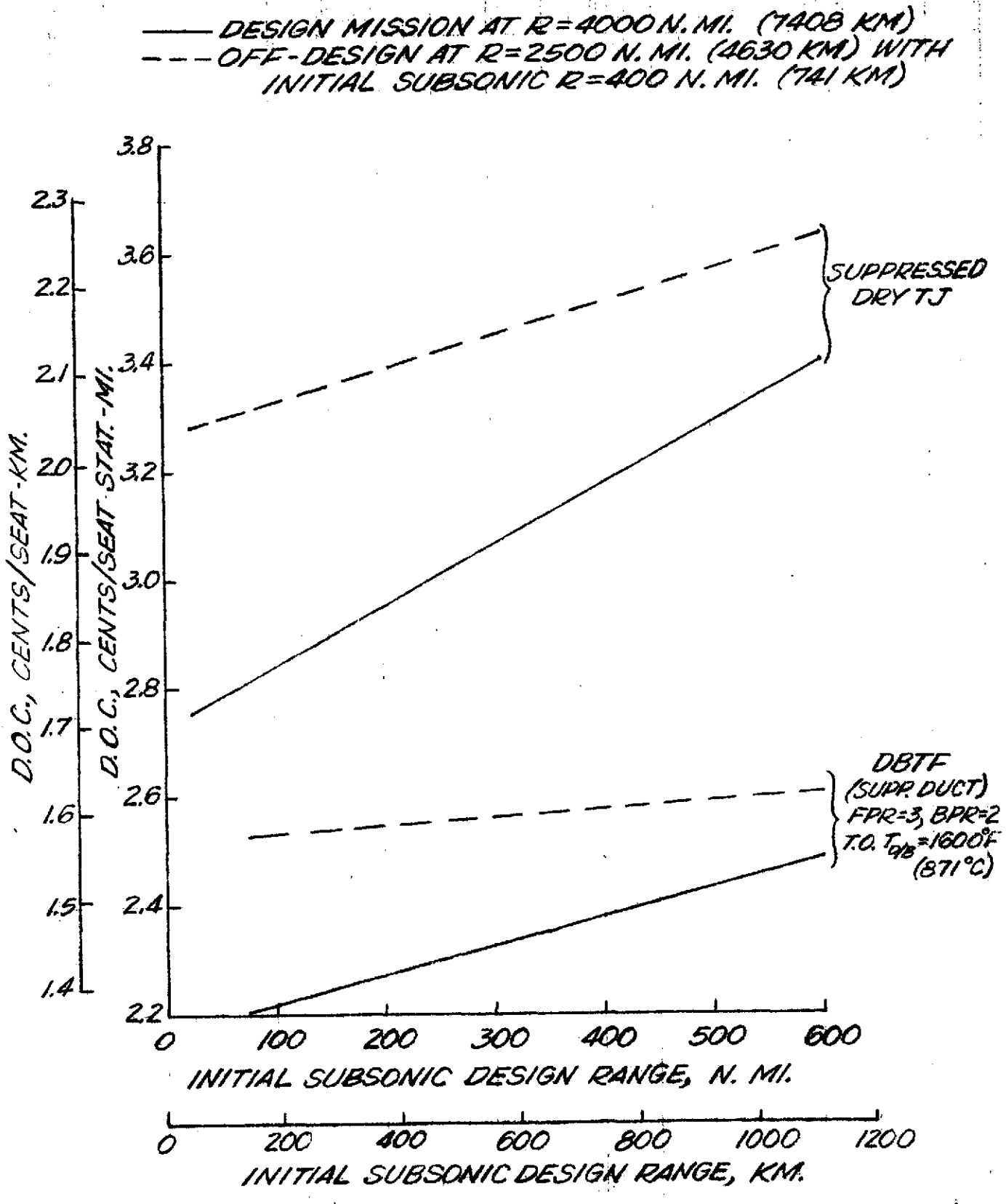

(B) DIRECT OPERATING COST. FUEL COST = 35 CENTS/GAL ($92.50/M³)

FIGURE 20- CONCLUDED.